

# GRADUATE AERONAUTICAL LABORATORIES CALIFORNIA INSTITUTE OF TECHNOLOGY

Experimental Investigation of an Arc Heater

by

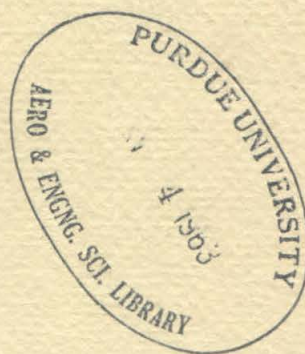
Marc L. Renard

HYPERSONIC RESEARCH PROJECT

Memorandum No. 64

March 15, 1962

Army Ordnance Contract No. DA-04-495-ORD-3231



Firestone Flight Sciences Laboratory

Guggenheim Aeronautical Laboratory

Karman Laboratory of Fluid Mechanics and Jet Propulsion

Pasadena

FIRESTONE FLIGHT SCIENCES LABORATORY  
GRADUATE AERONAUTICAL LABORATORIES  
CALIFORNIA INSTITUTE OF TECHNOLOGY  
Pasadena, California

Experimental Investigation of an Arc Heater

by

Marc L. Renard

HYPERSONIC RESEARCH PROJECT

Memorandum No. 64

---

March 15, 1962

Army Ordnance Contract No. DA-04-495-ORD-3231

  
Clark B. Millikan, Director



## ACKNOWLEDGMENTS

The author wishes to express his deep gratitude to Professor Toshi Kubota, under whose expert guidance this work was carried out and to whom he is indebted for numerous precious advice and hours of fruitful discussion, and to Professors Lees and Zukoski, members of his supervising committee. He acknowledges the help provided by the hypersonic laboratory staff in the installation of some experimental devices, and by the GALCIT 10 foot tunnel staff in the computations. Thanks are extended to Mrs. G. Van Gieson for typing the manuscript, and to Mrs. N. Kindig and Mr. J. Van Dijk for preparing the figures.

For their generosity and constant solicitude, special appreciation is expressed to the members of the Executive Committee and the Secretaries, in New York and Brussels, of the Belgian-American Educational Foundation, by whom the author was appointed a C. R. B. Graduate Fellow for 1960-1961.





## ABSTRACT

An electric arc heater, intended to provide a steady flow of high stagnation temperature gas (up to  $10,000^{\circ}\text{K}$ ) into a convergent-divergent nozzle, was designed at the GALCIT Hypersonic Laboratory.

Section 2 first gives a few preliminary calculations which have been made for the arc heater-nozzle combination, using argon, at stagnation pressures of 1 and 2 atm., and assuming equilibrium flow. In particular, the Mach number in the test section of a fixed nozzle will depend on the thermodynamic properties at the reservoir.

In the heater, the direct-current arc is axially constricted by a channel parallel to the gas flow. A description of the design and instrumentation is given in Sections 2 and 3.

For two series of experiments, using argon, the central electrode was either the cathode, as in the conventional arrangement, or the anode: both configurations were thoroughly investigated. Provided a sharp edge exists at the end of the flow constricting channel, the configuration with anode in the center was found to give, generally, a more stable functioning, with a voltage drop about twice as large, higher efficiency and thus higher average temperature for the same mass flow of gas, as compared to the case where the cathode is in the center. In the ranges of power (up to 13 Kw) and mass flow (up to 6.00 gr/sec) investigated, it was found that the best efficiency is obtained for a swirl close to the central electrode and large gas mass flows. When the anode is in the center, a long and narrow constricting channel leads to the optimal conditions. With the reversed polarities, the geometry of the downstream

channel is not very important.

Finally, a tentative explanation of the results is given, emphasizing in particular that the "anode in the center" case corresponds to a "long" arc, and the "cathode in the center" to a "short" one with poorer transfer of energy from the arc to the gas.

## TABLE OF CONTENTS

| PART                                                                                                                                        | PAGE |
|---------------------------------------------------------------------------------------------------------------------------------------------|------|
| Acknowledgments                                                                                                                             | ii   |
| Abstract                                                                                                                                    | iii  |
| Table of Contents                                                                                                                           | v    |
| List of Symbols                                                                                                                             | vi   |
| 1. The Arc Heater                                                                                                                           | 1    |
| 2. Design of Arc Heater                                                                                                                     | 2    |
| 2.1. Preliminary Calculations                                                                                                               | 2    |
| 2.2. Design of Arc Heater                                                                                                                   | 6    |
| 3. Preliminary Tests                                                                                                                        | 11   |
| 3.1. Tests A-7 and S-1                                                                                                                      | 11   |
| 3.2. Influence on the Injection Angle on the<br>Performance of the Heater                                                                   | 14   |
| 3.3. Conclusions from Preliminary Experiments                                                                                               | 16   |
| 4. Systematic Study of Efficiency, Arc Characteristics in<br>the Arc Heater as Functions of Geometry, Polarity,<br>and Mass Flow Parameters | 18   |
| 4.1. Introduction                                                                                                                           | 18   |
| 4.2. Experimental Set-Up                                                                                                                    | 18   |
| 4.3. Variables of the Problem and Experimental<br>Results                                                                                   | 18   |
| 4.4. Tentative Interpretation of Physical Results                                                                                           | 25   |
| 5. General Conclusions                                                                                                                      | 31   |
| References                                                                                                                                  | 33   |
| Appendix -- Equilibrium Speed of Sound in Ionizing<br>Argon                                                                                 | 34   |
| Tables                                                                                                                                      | 37   |
| Figures                                                                                                                                     | 47   |

## LIST OF SYMBOLS

|                   |                                                                                                                                              |
|-------------------|----------------------------------------------------------------------------------------------------------------------------------------------|
| a                 | adiabatic speed of sound                                                                                                                     |
| A                 | cross-section of the channel, or of the nozzle                                                                                               |
| c                 | specific heat                                                                                                                                |
| d                 | distance from central electrode tip to exit section                                                                                          |
| d'                | distance from central electrode tip to inner shoulder of arc chamber                                                                         |
| e                 | heat of ionization                                                                                                                           |
| E                 | electric field                                                                                                                               |
| f( )              | function of                                                                                                                                  |
| h                 | specific enthalpy (K. M. S.)                                                                                                                 |
| H                 | total specific enthalpy (K. M. S.)                                                                                                           |
| I                 | electric current in the arc                                                                                                                  |
| K                 | constant of law of mass action                                                                                                               |
| $l$               | depending on the case, distance from central electrode tip to exit section, or length of constricting channel; or heat of reaction, or liter |
| $\dot{m}$ or $m'$ | mass flow of gas (in gr/sec), or water (in liter/sec)                                                                                        |
| $\dot{M}$         | mass flow of gas per unit area of constricting channel                                                                                       |
| n                 | newton                                                                                                                                       |
| p                 | pressure                                                                                                                                     |
| P                 | power, or heat added per second in the heater                                                                                                |
| $\mathcal{P}$     | reduced net power input into the gas per unit area of throat section                                                                         |
| R                 | gas constant of argon                                                                                                                        |
| s                 | specific entropy (K. M. S.)                                                                                                                  |
| T                 | absolute temperature                                                                                                                         |



|          |                                                         |
|----------|---------------------------------------------------------|
| $u$      | velocity along axis of the channel                      |
| $v$      | velocity of the flow, or specific volume                |
| $V$      | voltage drop                                            |
| $x$      | abscissa along axis of the channel, or of the nozzle    |
| $\alpha$ | degree of ionization                                    |
| $\gamma$ | ratio of specific heats                                 |
| $\eta$   | efficiency of energy transfer process                   |
| $\theta$ | ratio of absolute temperature to ionization temperature |
| $\rho$   | density of gas                                          |
| $\phi$   | diameter of constricting channel                        |
| $> +$    | central electrode positive                              |
| $> -$    | central electrode negative                              |

#### Superscripts

|     |                 |
|-----|-----------------|
| $*$ | sonic condition |
| $-$ | average         |

#### Subscripts

|     |                                                    |
|-----|----------------------------------------------------|
| $A$ | of argon                                           |
| $+$ | of the ion                                         |
| $e$ | at equilibrium; or of the electron                 |
| $g$ | of the gas                                         |
| $i$ | of ionization                                      |
| $o$ | at $0^{\circ}\text{K}$ , or at $0^{\circ}\text{C}$ |
| $t$ | stagnation condition                               |



## 1. THE ARC HEATER

During the last few years, arc heating devices have been studied and used for many technical purposes connected with missile and space technology. They generate steady flows of gas at stagnation temperatures of thousands of degrees Kelvin, which are needed, among others<sup>1, 2</sup>, in the following applications:

(1) convergent-divergent expansion in a nozzle to achieve high velocities in the test section with high free stream temperatures for study of heat transfer and ablation rates (moderate reservoir pressure); or high velocities in the test section with low free stream temperatures for aerodynamic heating (high reservoir pressure).

(2) Supply of hot gases at high pressure and temperature for hypersonic wind tunnels.

(3) Magnetohydrodynamic studies.

(4) Low thrust propulsion devices.

(5) Study of flow of weakly ionized gases.

This work deals with the design and experimental study of the performance of a direct-current arc heater of the axial type, which means that the gas to be heated flows along a circular channel parallel to the path of the arc (Figure 1). The working fluid is argon at atmospheric pressure with a settling chamber and Laval nozzle connected to the exit section. The heater will be used to generate steady supersonic flows of high static temperatures.

It has to be stressed that there does not seem to be any reason to reject, a priori, the positive central electrode configuration, as has been done by previous workers.

## 2. DESIGN OF ARC HEATER

### 2.1. Preliminary Calculations

In order to obtain an estimate of various physical quantities occurring in the arc heater (Figure 1), and the nozzle flow, some preliminary calculations are made based on the one-dimensional flow of gases at very high temperatures.

For one-dimensional steady flows of a frictionless gas, at thermodynamic equilibrium, we have:

Continuity Equation:

$$\frac{d\rho}{\rho} + \frac{du}{u} + \frac{dA}{A} = 0, \text{ or } \rho u A = \text{constant} = \dot{m} \quad (1)$$

Momentum Equation:

$$\rho u du + dp = 0 \quad (2)$$

Energy Equation:

$$d\left(h + \frac{1}{2}u^2\right) = \frac{dP}{\dot{m}} \quad (3)$$

Equation of State:

$$p = p(\rho, h) \quad (4)$$

Here  $p$ ,  $\rho$ ,  $h$ ,  $u$  are the pressure, density, specific enthalpy and velocity of the gas, and  $A$  is the cross-sectional area of the channel, which is supposed to be given as a function of the distance along the channel,  $x$ .  $dP$  is the heat added to the gas per unit time. The heats of dissociation and ionization are not included in  $dP$ , but they are a part of the enthalpy  $h$ . Thus  $dP$  is not zero only in the heater. Define the

stagnation enthalpy  $H$ , as

$$H = \frac{1}{2} u^2 + h \quad . \quad (5)$$

Then

$$\dot{m} dH = dP \quad (6)$$

in the heater and

$$dH = 0 \quad (7)$$

elsewhere. By combining Eqs. 2 and 3, we obtain

$$\dot{m} T ds = dP \quad , \quad (8)$$

where  $s$  is the specific entropy,  $T$  the temperature. Thus the flow is isentropic outside the heater.\* For the isentropic flow,

$$(dp/d\rho) = a_e^2 \quad (9)$$

where  $a_e$  is the speed of sound at thermodynamic equilibrium. Then eliminating  $p$  and  $\rho$  between Eqs. 1, 2, and 9, we obtain

$$\frac{dA}{A} = \left( \frac{u^2}{a_e^2} - 1 \right) \frac{du}{u} \quad . \quad (10)$$

Thus  $A$  is minimum at  $u = a_e$ , or  $M_e = \frac{u}{a_e} = 1$ . The total mass flow rate through the channel is given by

$$\dot{m} = \rho_e^* a_e^* A^* \quad , \quad (11)$$

as in the perfect gas case. Also, from Eq. 7

$$H = h + \frac{1}{2} u^2 = \text{constant} = h_t \quad . \quad (12)$$

---

\* This is valid only for equilibrium flow or frozen flow. When the chemical reaction goes on at a finite rate, the entropy increases.



Hence the flow properties in a Laval nozzle are determined once the stagnation condition is given. For example, the stagnation condition can be specified by the pressure  $p_t$  and the enthalpy  $h_t$ . Then the corresponding entropy is obtained as  $s_t$ , and the flow properties are determined as functions of  $h$ :

$$\begin{aligned} p &= p(h, s_t) \\ \rho &= \rho(h, s_t) \\ u &= \sqrt{2(h_t - h)} \end{aligned} \quad (13)$$

The pressure and density of the gas is most easily obtained graphically on the Mollier chart of the working gas.  $a_e$  may be computed as indicated in the Appendix, with the assumption of the perfect gas behaviour for the atoms, the ions and the electrons individually, which is consistent with the method used to compute the Mollier chart<sup>2</sup>. The sonic condition is determined at the point where  $u = a$ . Then the area ratio  $A/A^*$  is obtained from  $A/A^* = \rho^* a^* / \rho u$ .

Across the heater,

$$h_t - H_{in} = (1/\dot{m}) P, \quad (14)$$

where  $H_{in}$  is the stagnation enthalpy of the incoming gas,  $h_t$  the stagnation enthalpy of the exhaust gas,  $P$  the total power transferred to the gas. For practical purpose,  $H_{in}$  is equal to the static enthalpy of the incoming gas, since its Mach number is very small. For a given nozzle, the total mass flow rate is a function of  $h_t$  and  $p_t$ ,

$$\dot{m} = \dot{m}(h_t, p_t) \quad (15)$$

Thus when  $p_t$  and  $P$  are given,  $\dot{m}$  and  $h_t$  are determined by Eqs. 14 and 15.

Eq. 15 may also be used to estimate  $h_t$  from the measurement of  $\dot{m}$  and  $p_t$ .

Table 1 gives the mass flow per unit area of the throat,  $\rho^* a^*$ , as a function of the reduced stagnation enthalpy for the two reservoir pressures  $p_t = 1 \text{ atm.}$  and  $2 \text{ atm.}$

In Figure 2, we plotted  $\rho^* a^*$ , as a function of  $h_t/RT_0$  for the two pressures:  $p_t = 1 \text{ atm.}$  and  $2 \text{ atm.}$  The dotted curves represent the same relation for the perfect, non-ionized gas of constant  $c_p$ .

On the same figure, curves of  $\rho^* a^*$  for constant  $\mathfrak{P} = \frac{P}{RT_0 A^*}$  have been drawn; they vary like  $\frac{1}{h_t/RT_0}$ , while  $\rho^* a^*$  for  $p_t = \text{constant}$ , vary like  $\frac{1}{\gamma h_t/RT_0}$  in the region of the perfect gas. The use of these curves is illustrated in the following numerical example.

### Numerical Example

Supposing the efficiency and the gross power input are known

Given  $P = 20 \text{ Kw}$   
and  $\dot{m}' = 1.235 \text{ gr/sec}$   
 $p_t = 1 \text{ atm.},$

then,

from Eq. 14:  $(h_t/RT_0) = 285.$

on Figure 2, the curve for  $p_t = 1 \text{ atm.}$  yields for  $(h_t/RT_0) = 285,$

$$\rho^* a^* = 35.5 \text{ kgmass/m}^2 \cdot \text{sec}$$

Hence:  $A^* = 0.348 \text{ cm.}^2$

(1) What is the new mass flow in the above nozzle if we double the reservoir pressure ( $p_t = 2$  atm.), and the net power input ( $P = 40$  Kw)? Then

$$\mathcal{G} = 20,000 \text{ (kgmass/m}^2 \text{ sec.)}.$$

The curve  $\mathcal{G} = 20,000$  intersects the mass-flow curve for  $p_t = 2$  atm. at the point  $(h_t/RT_o) = 274$ ,  $\rho^* a^* = 72.75$ . Hence, the mass flow with the nozzle  $A^* = 0.348 \text{ cm}^2$  and  $p_t = 2$  atm. is

$$m' = 2.53 \text{ gr/sec}$$

(2) With the same nozzle and the same  $P = 20$  Kw, what is the new mass flow if we double the reservoir pressure ( $p_t = 2$  atm.)?

Since,  $\mathcal{G} = 10,000$ , the point of the intersection of  $\mathcal{G} = 10,000$  with  $p_t = 2$  atm. yields:

$$(h_t/RT_o) = 107$$

$$\rho^* a^* = 93.25$$

Thus,  $m' = 3.25 \text{ gr/sec.}$

## 2.2. Design of Arc Heater

The arc heater is essentially made out of an arc-chamber, properly shaped, through which argon flows and is heated and eventually ionized.

It can be divided into four parts: the insulated head, the arc-chamber itself, the outer electrode cooling system, the anode and anode cooler (Figure 1).

## 2. 2. 1. Description and Design of Generator Blocks

### 2. 2. 1. 1. The Insulated Head and Distributor

The head is cylindrical and made out of micarta; it can be fixed by six nuts to the copper arc chamber. In its center is a hole which, with the one through the distributor disk, provides a smooth friction passage for the movable cylindrical electrode.

When the removable disk, d, is pushed into its seat, a small chamber remains, into which the gas is brought, through hole h. The gas then flows through injectors with an exit hole drilled normal to the axis. The gas can be injected into the arc-chamber with any degree of rotation, from  $0^{\circ}$  (radial injection) to  $90^{\circ}$  (tangential injection) by adjusting the orientation of injectors (Figure 3).

### 2. 2. 1. 2. Arc-Chamber

The arc-chamber itself is machined from a copper block. It has a cylindrical chamber, a conical contraction section and a cylindrical arc constricting section. The arc will strike the outer electrode somewhere along the cylindrical water-cooled constricting channel.

### 2. 2. 1. 3. Central Electrode

The central copper electrode is  $\frac{1}{2}$ " in diameter and is rounded at its end. It goes through the insulated head and the distributor disk, and is blocked at a minimum distance of  $1/4$ " from the shoulder in the arc-chamber.

The cooling system is composed of a copper tube ( $1/4$ " in diameter) inside the electrode, which is the water inlet; the space between



the inner and outer tubes provides the outlet.

### 2. 2. 2. Auxiliary Set-Ups

#### 2. 2. 2. 1. Electrodes

The central electrode is adjustable inside the chamber to position the electrode distance for stable arc operation; this is accomplished manually with a lever clamped on the central electrode.

The electrical power lead is connected to a copper block clamped around the tube; this provides the necessary good contact over a sufficient surface.

The other lead is connected to the copper frame which supports the arc-chamber.

#### 2. 2. 2. 2. Arc Starter

For conservation of the electrodes, the arc cannot be started by bringing into contact and moving away the central and the outer electrode. Instead, it was decided to use the exploding wire technique to start the arc. A very thin piano wire is introduced into the chamber through a tiny hole, along which a sufficient contact with the wire is assured. It is held in position through a strongly compressed teflon piece; the latter prevents also any leakage. The switch-on current makes the wire melt instantaneously and creates a local overheating and ionization, which enables the principal arc to start (Figure 5).



### 2.2.2.3. Water Connections

At the central electrode, the water goes through the inner tube. At the outer electrode, the incoming water flows first around the terminal part of the constricting channel.

### 2.2.3. Instrumentation

Since the purpose of the experiment is to determine the efficiency of the energy transfer process to argon through the arc, the instrumentation described below was provided. The set-up is illustrated clearly by the diagram of Figure 6.

#### 2.2.3.1. Water Cooling Circuits

Two flowmeters, thoroughly calibrated, measure respectively the total flow through the central and outer electrodes, and the flow through the central electrode. The arc-chamber flow is determined by difference.

To fix an order of magnitude of the water flows involved, a preliminary test gave:

central:  $m' = 0.1252 \text{ l/sec.}$

outer:  $m' = 0.166 \text{ l/sec.}$

The inlet and outlet temperatures, for both electrodes, are measured by thermopiles (copper-constantan), placed in micarta blocks at the inlets and outlets; the readings being made on a Leeds Northrup K-2 potentiometer. To isolate the thermopiles electrically from the electrodes, water connections between the block and the electrodes were made out of plastic tubing and a short length of copper tubing at

the micarta block end, the latter being electrically grounded.

#### 2.2.3.2. Gas Circuit

A Fisher and Porter Triflat flowmeter, with a stainless steel ball float, was used to measure the mass flow of argon. Its calibration curve was computed for 2 upstream pressures: 50 and 60 psi. A pressure gage measures the pressure in the arc chamber.

#### 2.2.3.3. Electric Circuit

The electric power input was measured by reading:

- $V_{\text{arc}}$  , voltage drop across the arc

- $I_{\text{arc}}$  , arc current .

The stabilization resistance was kept at 2.9 ohms. In the range of power, 0 - 13 Kw, the current could be adjusted by regulation of the output voltage of the D. C. generators.

### 3. PRELIMINARY TESTS

#### 3.1. Tests A-7 and S-1

From the first two tests on the arc heater, we were able to draw some qualitative conclusions and, therefrom, were induced to modify some experimental devices in order to obtain significant results.

The details of the instrumentation and some characteristic results are recorded in Table 2.

The efficiency of the energy transfer process to the gas is defined by the ratio of the power added to the gas,  $P_{\text{gas}}$  to the power dissipated in the arc,  $P_{\text{input}}$ :

$$\eta = \frac{P_{\text{gas}}}{P_{\text{input}}} .$$

$P_{\text{gas}}$  is measured by an energy balance

$$P_{\text{gas}} = P_{\text{input}} - P_{\text{electrodes}} ,$$

where  $P_{\text{electrodes}}$  is the power absorbed by the cooling circuit. It is determined by careful measurements of the water mass flow and the temperature rise through the electrodes circuit.  $P_{\text{input}}$  is simply the product of the voltage drop across the arc  $V_{\text{arc}}$  by the arc current  $I_{\text{arc}}$ . Direct reading of the two last quantities enables the arc characteristic to be drawn. Thus

$$\eta = 1 - \frac{P_{\text{electrodes}}}{P_{\text{input}}} .$$

Finally, the average temperature of the gas,  $\bar{T}_g$ , can be obtained from Figure 7, which gives  $\bar{T}_g$  as a function of the net power input per unit

mass flow ( $P_{\text{gas}}/m'$ ) or ( $\eta P_{\text{input}}/m'$ ).

In these first two tests, we used the block described in the previous section. However, the thermometric measurements in the water-cooling circuit were made with a Brown self-balancing potentiometer and single non-grounded iron-constantan thermocouples. Owing to the smallness of the difference in temperatures involved it appeared that any hope for accuracy was somewhat illusory. Only some orders of magnitude and qualitative conclusions could be obtained.

The gas was injected with an angle of  $90^\circ$  (Figure 3) in both cases, and the distance  $d$  (Figure 5) was varied around a position (about 1 diameter from the inner shoulder) which gave enough stability without excessive overheating of the electrodes. The power level and the mass flow were kept at moderate values (not exceeding 4 Kw and 1.4 gr/sec). The pressure in the chamber was seen to be atmospheric within a very few per cent.

The most striking fact revealed by experience is the complete difference in behaviour of the arc with different polarities for identical geometry, angle of injection and mass flow.

When the central electrode is positive (A-7), the arc turns out to be fairly stable, even with copper electrodes. It undoubtedly strikes the cathode along the sharp edge XX (Figure 5), where, after a few minutes, an intense erosion occurs. Once the copper in XX is burning, one observes appreciable fluctuations of voltage drop across the arc and of brilliancy, the burned copper giving a green color to the jet. No damage is seen on the central electrode (anode). To avoid this erosion, one thinks at first to suppress the concentration of field in XX



by rounding off the sharp edge. But, as will appear more clearly at the end of the next section, the existence of a sharp edge at the exit section is precisely essential to that functioning with anode in the center: when the damaged part was rounded off, the arc became completely unstable, and blew itself off even with such a large starting voltage as 200 V. Since in conventional designs<sup>2, 6</sup>, the conical part of the arc chamber is already the convergent part of the nozzle, followed by the throat and the divergent section having no sharp edge, this could presumably explain why the "anode in the center" was found an unstable configuration, and previous experimentators only retained the "cathode in the center" case.

The efficiency, varying from 50 per cent to 70 per cent, was of the same order of magnitude as in Cann's data<sup>1</sup>.

With that polarity, the voltage drop, of about 50 V, is found to be insensitive to the distance  $d$ , but the arc quickly becomes more unstable, the more  $d$  is increased.

When the central electrode is negative (S-1), the arc is more unstable, in current as well as in voltage. This will be seen in all our experiments. Furthermore, the central electrode, made out of copper, is readily damaged: the arc strikes the cathode around the center of the tip, digging a crater and projecting drops of copper in the flow. Furthermore, the fact that XX was not damaged at all, that a very slight erosion was seen on the inner shoulder and that the arc looked as being "inside" gave a first experimental evidence that the arc was striking along the "short" path going from the tip of the central electrode to the wall of the arc-chamber, which is what occurs in the conventional



polarity configuration<sup>2, 6</sup>. Accordingly, the voltage drop across the arc (about 30 V) was reduced by a factor of the order of 2. At this stage, no measurements of efficiency were made. However, with that reduced voltage drop and small heating region, one should expect the efficiency to be smaller, which is indeed the case. Finally,  $V_{\text{arc}}$  is seen to increase slightly with increasing  $d$ .

Tests A-7 and S-1 stress the necessity for very heat-resistant electrodes and more accurate measurements of the temperature increase of the cooling water. The latter is a twofold requirement: in sensitivity of the reading; and in appropriate insulation of the thermocouple, which is introduced in the water circuit, while the water itself is in contact with conducting parts of the electric circuit.

Hence we modified the set-up as described in Section 2.2.

In the succeeding tests, a ring of 2 per cent thoriated tungsten was put at the exit section (Figure 8), to prevent the sharp edge XX from being damaged by the arc striking. It was not eroded in the course of experiment. Eventually, the whole tube of the constricting channel was made out of tungsten, but this turned out to be a useless precaution. Thoriated tungsten was used also for the 60°-conically shaped central electrode tip (Figure 9).

### 3.2. Influence of the Injection Angle on the Performance of the Heater

The tests reported in Table 2 (S-11; S-22; S-26; O-11; O-12), the results of which are given on Figures 11 to 13, consisted essentially of measuring, by the method described at the beginning of this section, the efficiency of the energy transfer process into the gas and in obtaining

the arc characteristic for:

- (1) various "degrees" of swirl (variation of the direction of the injection velocity: See Figure 3)
- (2) for a fixed degree of injection, various mass flows
- (3) for a fixed mass flow, various values of the current or, subsequently, of the gross power input ( $P_{\text{input}}$ )
- (4) the two configurations: "anode in the center", noted  $> +$  ; "cathode in the center" noted  $> -$  .

As previously, the pressure in the arc chamber was very slightly above atmospheric pressure. The distance  $d$  from the tip of the central electrode to the exit section was kept constant at around 2 inches when the anode is in the center, at 1.6 inches in the opposite case. These distances gave stable functioning points over the whole range of power investigated. As to the injection angle, the main feature is that, with radially injected gas, the arc is very unstable, and leads to poor efficiencies: in the worst case (cathode in the center), an excessive overheating of the distributor could be seen. With a  $90^\circ$  or  $45^\circ$  angle of injection, the arc is very stable. As could be expected, the  $45^\circ$  injection gives slightly better results than the  $90^\circ$  one, since the first angle corresponds to jets very close to the central electrode (Figure 3), while, for the second one, the gas stream collides against the walls of the chamber.

Regarding the influence of the other factors on the efficiency and arc characteristic, a quantitative confirmation of the higher efficiency and voltage drop, when the anode is in the center, was obtained, as well as their evolution with increasing mass flow and power input.

In the experimental data of Figures 11 to 13, when the electrodes were allowed to reach their equilibrium temperature, the results were reproducible within one point of efficiency.

### 3.3. Conclusions from Preliminary Experiments

By observing the experimental data and by comparing them, several conclusions can be drawn, which will guide us in further systematic study of the efficiency. It can be stated:

(1) Whatever the polarity, the efficiency decreases with increasing gross power input, for given injection and mass flow; the efficiency increases with increasing mass flow, for given injection and power input. It is optimum for  $45^\circ$  injection (slightly better, more constant than  $90^\circ$ ). The  $0^\circ$  injection (radial) has to be rejected.

(2) For the efficiency, the "positive central electrode" configuration is much more advantageous, all other factors being equal.

(3) Whatever the polarity,  $V_{\text{arc}}$  is nearly constant, or increases slowly with increasing currents, for given injection angle and mass flow. It shifted upwards, a few volts or less, with increasing mass flow (0.92 to 1.98 gr/sec), for given injection angle. It decreased very slightly with increasing angle of injection above  $45^\circ$ , for given mass flow.

(4) The "positive central electrode" configuration presents a voltage drop which is on the average of about 40 V, while the cathode central electrode configuration gives only 25 V. Consequently, it seems that the first case will be more advantageous for maximizing the transfer to the arc.

(5) As to the average gas temperature, for given mass flow and power input,  $\bar{T}_g$  being a monotonously increasing function of the ratio  $\frac{\eta P_{\text{input}}}{m'}$ , varies like  $\eta$ ; but for increasing  $m'$ , the effect of  $(1/m')$  in the ratio is much stronger than the corresponding increase in efficiency, so that  $\bar{T}_g$  decreases.



## 4. SYSTEMATIC STUDY OF EFFICIENCY AND ARC CHARACTERISTICS IN THE ARC HEATER AS FUNCTIONS OF GEOMETRY, POLARITY, AND MASS FLOW PARAMETERS

### 4.1. Introduction

The purpose of this experimental study was to proceed to an investigation of the influence, on the efficiency and arc characteristic, of various parameters of geometry and mass flow, for gross power input up to 13 Kw.

### 4.2. Experimental Set-Up

It is fundamentally the same as the one described before: the same central electrode with tungsten tip, the micarta head and gas distributor were kept; it should be noted that the angle of injection was kept at the fixed value  $45^{\circ}$ , which previous experiments have proved sufficiently to give the optimum efficiency, all other factors being held constant.

A copper block, with  $30^{\circ}$  inclined walls and an exit section of  $\phi = \frac{1}{2}$ ", provided the arc-chamber, fixed to the micarta head (Figure 1). To this block, various removable constriction sections can be adapted (Figure 10). The tube forming the walls of the last section, where the arc most likely strikes, is of tungsten instead of copper.

### 4.3. Variables of the Problem and Experimental Results

The dependent variables of the problem are as before:

the efficiency,  $\eta = \frac{P_{\text{gas}}}{P_{\text{input}}}$ , and the voltage drop across the arc,

$V_{\text{arc}}$ .

They are functions of:

- (1) The ratio,  $l/\phi$ , of the length of the arc constricting channel to the diameter of its section;
- (2) The diameter,  $\phi$ , of the constricting channel;
- (3) The magnitude of the mass flow  $m'$ ;
- (4) The polarities: central electrode positive being noted  $> +$   
central electrode negative being noted  $> -$  ;
- (5) The power input.

The position of the central electrode, given by  $d'$  on Figure 10, is not a parameter: it was chosen equal to  $\frac{1}{2}$ ", by a compromise between the necessity for a stable arc (arc unstable for large  $d'$ , especially for  $> -$ ), and for not overheating the electrodes if brought too close together, or shortening the arc excessively.

An interesting compound parameter in the problem is the mass flow per unit area of the cross section of the outer electrode. We define a "mass factor":  $\mathcal{M} = (m'/A)$ , where

$m'$  = mass flow of gas, in gr/sec

$A = \pi (\phi^2/4) =$  area of cross section, in inches<sup>2</sup>.

$\mathcal{M}$  is in some sense the "image" of the velocity through the circular channel (proportional to the exit velocity, if  $\rho_{\text{exit}}$  was constant).

Having in mind the example, of say, pneumatic circuit-breakers, we may predict that above some critical value of  $\mathcal{M}$ , the arc will not be maintained in a stable position, or will just be blown away. The latter occurs for  $\mathcal{M} = 122$ , the polarity  $> +$ , and the "long" arc  $l/\phi = 8$ , whatever the starting voltage up to 250V.



#### 4.3.1. Particular Values Chosen

(1) for  $\phi$ :  $\frac{1}{2}$ , 0.354,  $1/4$  (inches) giving sections,

$$\text{with } A = \frac{\pi(1/4)^2}{4} \text{ inches}^2,$$

$$4A \quad 2A \quad A$$

(2) For  $l/\phi$             1        2        4        8

(3) Polarities:  $> +$  and  $> -$

(4) Values of  $m'$ : 6, 4.24, 3, 2.12, 1.50, 1.06 (gr/sec)

Values of  $\dot{M}$  are multiples of each other. They vary between 5.4 and 122 gr/sec x inches<sup>2</sup>.

Table 4 gives a listing of the experiments performed, with their index number, which for clarity is omitted on the corresponding graphs.

#### 4.3.2. Experimental Results

Experimental results are given graphically in Figures 14 to 29. For compactness, no curves have been drawn here; but the conclusions which follow are based on separate graphs plotted for each case.

Each figure corresponds to one value of  $l/\phi$  (in decreasing order), one polarity ( $> +$  before  $> -$ ), and various mass flows and diameters; in each case are reported  $\eta = f(P_{\text{input}})$  and  $V_{\text{arc}} = f(I_{\text{arc}})$ .

Furthermore, for a typical example of variation of these quantities with  $l$  only, all other factors being constant, the reader should refer to Figure 30 and Figures 32 to 35.

The maximum and minimum values obtained in the whole set of experiments are recorded below. It emphasizes the fact that very large

changes in  $\eta$ ,  $V_{\text{arc}}$  are obtained when changing the polarities, mass flow and geometry; furthermore, extremal values of these quantities appear, if not always very pronounced, for extremal values of the parameters.

### A. Arc Voltage, $V_{\text{arc}}$

#### I. $> +$ : Central Electrode Positive

##### (a) Maximum Value

$V = 150.5 \text{ V}$  at  $63\text{A}$ ;  $P_{\text{input}} = 9,482 \text{ w}$ ;

$\eta = 84 \text{ per cent}$ ;  $\bar{T}_g = 3,650^\circ\text{K}$ ;  $m' = 4.24 \text{ gr/sec}$ ;

$\mathcal{H} = 86.4$ ;  $l/\phi = 4$ ;  $\phi = 1/4''$ .

The voltage drop was observed to be greater for

$l/\phi = 8$ ;  $\phi = 1/4''$ , but was unstable.

##### (b) Minimum Value

$V_{\text{arc}} = 26.5 \text{ V}$  at  $140.5 \text{ A}$ ;  $P_{\text{input}} = 5,710 \text{ W}$ ;  $\eta = 44.2 \text{ per cent}$

$\bar{T}_g = 2,950^\circ\text{K}$ ;  $m' = 1.06 \text{ gr/sec}$ ;  $\mathcal{H} = 5.4$ ;  $l/\phi = 1$ ,  $\phi = \frac{1}{2}''$

#### II. $> -$ : Central Electrode Negative

##### (a) Maximum Value

$V_{\text{arc}} = 79.75 \text{ V}$  at  $148\text{A}$  ( $11,803 \text{ w}$ );  $\eta = 62 \text{ per cent}$ ;

$\bar{T}_g = 2,300^\circ\text{K}$ ;  $m' = 5.00 \text{ gr/sec}$ ;  $\mathcal{H} = 122.24$ ;  $l/\phi = 8$ ,  $\phi = 1/4''$

(b) Absolute Minimum Values

$$V_{\text{arc}} = 18.25 \text{ V at } 143.5 \text{ A ; } P_{\text{input}} = 2,942 \text{ W ;}$$

$$\eta = 25.6 \text{ per cent ; } \bar{T}_g = 1,820^\circ \text{K ; } m' = 1.06 \text{ gr/sec ;}$$

$$\mathcal{H}C = 10.8 ; \ell/\phi = 1 ; \phi = 0.354'' \text{ (same result for } \phi = 1/4'')$$

B. EfficiencyI. > + : Central Electrode Positive(a) Maximum

$$\eta = 87.9 \text{ per cent ; } P_{\text{input}} = 8,200 \text{ w ;}$$

$$V_{\text{arc}} = 132.25 \text{ V ; } I = 62 \text{ A ; } \bar{T}_g = 1,430^\circ \text{K ; } m' = 3.00 \text{ gr/sec ;}$$

$$\mathcal{H}C = 61.12 \text{ (equivalent results for } \mathcal{H}C = 86.4 ; \mathcal{H}C = 122.4$$

could not be obtained, the arc blowing itself off)

(b) Minimum

$$\eta = 41.0 \text{ per cent ; } P_{\text{input}} = 1.831 \text{ W ; } V_{\text{arc}} = 28 \text{ V ;}$$

$$I = 186 \text{ A ; } \bar{T}_g = 3,830^\circ \text{K ; } m' = 1.06 \text{ gr/sec ; } \mathcal{H}C = 5.4 .$$

II. > - : Central Electrode Negative(a) Maximum

$$\eta = 83.7 \text{ per cent ; } P_{\text{input}} = 5,372 \text{ W ; } V_{\text{arc}} = 79 \text{ V ;}$$

$$I = 68 \text{ A ; } \bar{T}_g = 1,500^\circ \text{K ; } m' = 6.00 \text{ gr/sec ; } \mathcal{H}C = 122.24 ;$$

$$\ell/\phi = 2 \text{ and } \phi = 1/4'' \text{ ( } \ell/\phi = 1 \text{ was not experimented)}$$

(b) Minimum

$$\eta = 14.7 \text{ per cent ; } P_{\text{input}} = 3.608 \text{ W ; } V_{\text{arc}} = 20.5 \text{ V ;}$$

$$I = 176 \text{ A ; } \bar{T}_g = 980^\circ \text{ K ; } m' = 1.06 \text{ gr/sec ; } \mathcal{H} = 5.4 ;$$

$$l/\phi = 8 ; \phi = \frac{1}{2}''$$

4.3.3. Conclusions

At least in the range of variation of the different quantities, the results of the experiments show the choice of the parameters to be made in order to get the best  $\eta$ , largest  $V_{\text{arc}}$  and highest  $\bar{T}_g$ . (See Table 4.)

A first condition for high efficiency is, as stated before, an injection with a swirl close to the central electrode.

The comparison of the two polarity cases:  $> +$  (central electrode positive) and  $> -$  (central electrode negative) clearly proves that for best  $\eta$ ,  $V_{\text{arc}}$ ,  $\bar{T}_g$ ,  $> +$  has to be preferred to  $> -$ .

Whatever the polarity, one must take the largest possible values of the mass flow per unit area  $\mathcal{H}$  (Thus: large mass flows and small diameters of the constriction section), but always considering the need for a stable arc (See Section 4.3.) and sufficient temperatures at the exit. Large values of  $l$  have to be chosen for optimum efficiency and large voltage drop when the anode is in the center ( $> +$ ); small values of  $l$  with the reversed polarities ( $> -$ ). The reason for that difference will be seen in what follows.

Now, after analyzing the experimental data, it was possible to

summarize, as is done synthetically in Table 4, the influence of the various parameters on  $\eta$  and  $V_{\text{arc}}$ . This table outlines the general trend of the variables with the variation of the parameters, to which a very few exceptions may exist (in particular, jumps in position, and thus in voltage drop, can occur for the short arc).

Some further comments have to be made. First, experiments confirm what is expected intuitively: that the efficiency and the voltage drop vary together in the same sense. Paragraph 4 of this section gives evidence that an important voltage drop occurs in the positive column of the arc, at least in the case  $> +$  : so, the larger the voltage drop, the larger the ionization and heating region, and the larger the efficiency.

As stated above, for given geometry and mass flow, the efficiency is seen to be better when the anode is in the center for the same power input, and the voltage is higher by a factor of about 2, for the same current.

The configuration  $> +$  is much more stable, in general, than  $> -$ . This difference in behavior does not appear clearly at high mass flow, and can even be reversed at very high values of  $\dot{M}$ . For the configuration  $> +$ ,  $(dV/dI)$  is positive, while for the second one,  $(dV/dI)$  is negative for moderate currents, and eventually slightly positive for very high currents.

For both polarities, efficiency and voltage drop decrease with the power input, in general, increase with increasing mass flow and decreasing diameter, and always increase with increasing  $\dot{M}$ . It can be remarked that for the configuration  $> -$ ,  $V_{\text{arc}}$  increases slightly



with increasing diameter at small mass flows, which was attributed to a local overheating and choking at small diameters, causing a "thermal" drop in voltage; while at large mass flows,  $V_{\text{arc}}$  goes down with the diameter because the increased flow speed sweeps the arc downstream. Finally, in the central-electrode-positive  $> +$  configuration, the efficiency and arc voltage go up with the length  $l$ , which corresponds closely to the length of the arc, and thus the heating region. In the  $> -$  configuration, the arc does not extend over the whole length of constricting section, and  $l$  is just a useless length of "cooling channel", so that  $\eta$  should indeed decrease with  $l$ , while  $V_{\text{arc}}$  remains constant.

#### 4.4. Tentative Interpretation of Physical Results

##### 4.4.1. Physical Model

In the static case, the potential distribution in the electric arc is represented by Figure 4, giving  $V = V(x)$ ,  $x$  being the distance "along" the arc. Since the regions where the cathode and anode voltage drop occurs are small, the length of the positive column can be equated, with negligible error, to the total length of the arc.

We distinguish three regions:

(1) Cathode-drop region, of very high positive ion-space density, with  $V_c$  "large".  $V_c$  may be taken, at atmospheric pressure, as the first ionization potential = 15.76 V.

(2) Positive column, where  $E$  is constant and depends on the nature of the gas, the pressure and the current. The voltage drop in the positive column is then proportional to the length of the arc.

(3) Anode-drop region, of very high electron-space density,



with  $V_a$  smaller than  $V_c$ .

To that physical situation, we superimpose a flow pattern of which we consider only the axial effects (along the axis of the column) on the electric phenomena: we call the effects of the flow "mechanical".

We are now trying to define roughly the degree of the coupling between the "electrical" and "mechanical" flows. Accordingly, we compare the ion- and electron- drift velocities to the flow velocity.

(1) The average conditions considered are

$$\bar{T} = 3,000^\circ\text{K}, \quad p = 1 \text{ atm}; \quad m' = 3.00 \text{ gr/sec}; \quad \phi = 0.354 \text{ inches.}$$

Plotting  $V_{\text{arc}} = f(l)$  for  $I = 100 \text{ A}$ ,  $p = 1 \text{ atm}$ , we find

$$\frac{dV_{\text{arc}}}{dl} = \text{constant} = \bar{E} = 10 \text{ V/cm.}$$

The ion drift velocity is<sup>5</sup>:

$$\bar{v}_+ = K_+ \bar{E}, \quad \text{and} \quad K_+ = \frac{e L}{m \bar{c}}. \quad \text{Then}$$

$$\bar{v}_+ = 45.5 \text{ cm/sec.}$$

The electron drift velocity is

$$\bar{v}_e = K_e \bar{E}$$

By Compton's formula<sup>5</sup>:

$$K_e = \frac{271,000 \lambda_{10} (273/T)^{\frac{1}{2}}}{\left\{ 1 + \left[ 1 + 1; 106,000 M \lambda_{10}^2 (E/p)^2 \right]^{\frac{1}{2}} \right\}^{\frac{1}{2}}}$$

where

$\lambda_{10}$  = electron mean free path at 1 mm Hg.,  $273^\circ\text{K}$

$M$  = molecular weight of the gas

$\bar{E}$  = electric field in V/cm

$p$  = pressure in mm Hg

Thus  $\bar{v}_e = 133,350 \text{ cm/sec.}$

The "flow velocity" is the average velocity in the constricting channel:

$$\bar{v}_{\text{flow}} = 28,460 \text{ cm/sec.}$$

The velocity ratios of the flow on the ions and electrons are respectively

$$\frac{\bar{v}_{\text{flow}}}{\bar{v}_+} = 626 \quad \text{while} \quad \frac{\bar{v}_{\text{flow}}}{\bar{v}_e} = 0.2135 ,$$

and one should then expect the ions to be strongly affected by the flow, and the electrons very little.

(2) In the general case, when one does not assume any particular value for  $\bar{v}$ ,  $\bar{\rho}$ ,  $S$ ,  $\bar{T}$ ,  $\bar{E}$ , one writes

$$\frac{\bar{v}_{\text{flow}}}{\bar{v}_+} = \frac{1}{\bar{E}} \frac{m' / \bar{\rho} S}{e / m \bar{c}} .$$

Since

$$\bar{c} \div \sqrt{\bar{T}} , \quad \lambda \div \frac{1}{\bar{\rho}} ,$$

$$\frac{\bar{v}_{\text{flow}}}{\bar{v}_+} = \text{constant} \cdot \frac{\mathcal{H}}{\bar{E}} \sqrt{\bar{T}} ,$$

so that it can be stated that the action of the flow on the ions will be increased with

increasing  $\mathcal{H}$  (large mass flow or/and small diameter)

increasing temperature  $\bar{T}$

decreasing field .

On the other hand, if in the computation of  $\bar{v}_e$  by Compton's formula,  $1$  is neglected compared to about 10, then  $\bar{v}_e \sim \frac{1}{\sqrt{\bar{E}}}$  , so

that

$$\frac{\bar{v}_{\text{flow}}}{\bar{v}_e} = \text{constant} \cdot \frac{M}{\sqrt{E}} \bar{T}.$$

Hence, fixing  $\bar{v}_{\text{flow}}$ , the relative importance of the "electronic" and "ionic" behavior of the arc is estimated by

$$\frac{\bar{v}_e}{\bar{v}_+} = \text{constant} \frac{1}{\sqrt{E} \bar{T}}.$$

#### 4.4.2. Comparison of "Central Electrode Positive" and "Central Electrode Negative" Functionings

A schematic representation of the "central electrode positive" and "central electrode negative" configurations can be found in Figure 31. In the flow field, there are three possible regions of concentration of the electric field: A, central cathode tip; B, inner shoulder; C, exit section edge.

##### A. "Central Electrode Positive" Configuration

It can be argued that the arc will strike along either AB (from the tip to the inner shoulder) or AC (from the tip to the exit section edge). Because of the strong coupling between flow and ions, the ions can easily be carried downstream in the direction of their own drift velocity, while the electrons going upstream do not "see the flow".\* One should then expect a strong electric field, and thus voltage drop, in order to

---

\* This was sufficiently proved experimentally: the inner shoulder remaining sharp, the edge of the exit section had been rounded off. In the "central electrode positive" configuration, the arc could not be maintained for any value of the current.

maintain the arc attached to the edge C. The anode-drop of the electrons, furthermore, occurring in a "dead-water" region of the flow should be small. From what has been said in the preceding paragraph, one can predict quantitatively:

the larger  $\mathcal{H}$ , the larger becomes the voltage drop, and

for very large velocities, the arc is blown away, whatever the starting field.

If  $V_a$ ,  $V_c$  are taken as constant, increasing the length  $\ell$  results in a corresponding increase of the voltage drop in the positive column, so that

$$V_{\text{total}} = V_{\text{an}} + V_{\text{cath}} + \left( \frac{d V_{\text{total}}}{d \ell} \right) \ell$$

#### B. "Central Electrode Negative" Configuration

The ions, strongly affected by the mechanical action of the flow, this time have a small drift velocity directed upstream of the flow. It seems probable that they will take the shortest path BA from the inner shoulder to the central electrode tip of the order of  $\frac{1}{2}$ "("short" arc configuration). The voltage drop at the cathode now occurs in the "dead-water" region of the flow where the motion of the ions is easier; hence a smaller average voltage drop. Furthermore, this causes the "ionic" character of the discharge to be less important:  $\bar{v}_{\text{flow}}/\bar{v}_+$  should decrease, which for constant  $\mathcal{H}$  implies

$\bar{T}$  larger, improbable, since the flow does not stay long enough in the heating region;

$\bar{E}$  large, which effectively is the case. (Of the order of 23 V/cm).

Finally, the efficiency should drop with  $\ell$ , the region downstream



of B being a useless "cooling channel". The voltage drop across the arc must increase with  $\mathcal{H}$  and depends on the downstream geometry only through the influence of  $\phi$  on the velocities around the inner shoulder B, and not through  $l$ . This point will be checked now.

### C. Voltage Drop in the Positive Column

In order to check the validity of the above representation, we plotted  $V_{\text{arc}} = f(l)$ ,  $l$  being the length of the positive column, for a given value of the polarity, the diameter, the mass flow, and the current (Figures 32 to 35). For the "central electrode positive" configuration,  $V_{\text{arc}} = f(l)$  is indeed linear, which justifies a posteriori the assumptions:  $V_a$ ,  $V_c$  constant and  $V_{\text{arc}} = V_{\text{total}} = V_{\text{an}} + V_{\text{cath}} + \bar{E}l$ , where  $\bar{E} = \text{constant} = (dV/dl)$ .  $\bar{E}$  is seen to increase strongly with increasing  $\mathcal{H}$ , but for high values of  $\mathcal{H}$  and  $I$ , the arc is not maintained. For the "central electrode negative" configuration,  $V_{\text{arc}} = f(l)$  is practically constant, which shows that the length of the positive column does not vary with the length of the constricting channel: indeed, the arc, striking along the "short" path is unaffected by what is downstream.

## 5. GENERAL CONCLUSIONS

This study determines the influence of the various geometric parameters, mass flow, and polarity on the efficiency of an arc heater of the axial type at low power level.

Provided a sharp edge exists at the exit section of the constricting channel, the "central electrode positive" configuration gives better results in any respect, except that the "long" arc is blown away more easily for large values of the mass flow per unit area. It was found in particular that the efficiency and the voltage drop across the heater are always larger, compared to the case where the cathode is in the center.

When the central electrode is positive, the efficiency is seen to increase slightly with the length of the constricting channel, and to increase with increasing mass flow per unit area  $\mathcal{M}$ . With increasing  $\mathcal{M}$ , the voltage drop increases strongly, and it varies linearly, with a large slope, with the length of the channel ("long" arc configuration). Furthermore, it increases with increasing current ("positive" arc characteristic).

When the central electrode is negative, the efficiency decreases for longer channels and increases with  $\mathcal{M}$ . The voltage drop increases with  $\mathcal{M}$ , remains unaffected by the length of the downstream channel ("short" arc configuration), and decreases with increasing current ("negative" arc characteristic). However, further investigation is needed to check whether significant changes in behaviour could not occur if the arc is forced, mechanically and/or electrically, to strike



further downstream.

The above investigation stresses the advantage of having the anode in the center, a swirl close to the central electrode, and a long and narrow constricting channel, which presumably is completely filled by the plasma of the positive column.

## REFERENCES

1. Cann, Gordon L. : Energy Transfer Processes in a Partially Ionized Gas. GALCIT Hypersonic Research Project, Memorandum No. 61, June 15, 1961.
2. Westinghouse Electric Corporation: Description of Arc Heater System. Arc Heater Symposium of the Westinghouse Electric Corporation, East Pittsburgh, Pennsylvania, September, 1960.
3. Cann, Gordon L. : Mollier Chart for Argon. Plasmadyne Corporation, Santa Ana, California, Air Force Office of Scientific Research, Contract No. AF 49(638)-54, February 20, 1959.
4. Mueller, James N. : Equations, Tables and Figures for Use in the Analysis of Helium Flow at Supersonic and Hypersonic Speeds. NACA Technical Note 4063, September, 1957.
5. Cobine, James D. : Gaseous Conductors. Dover Publications, Inc., New York, N. Y., 1958.
6. Clayden, W. A. : Recent Research in the ARDE Low Density Wind Tunnel with a Plasma Jet Heater. Rarefied Gas Dynamics, edited by L. Talbot, p. 715, Academic Press, New York, N. Y., 1961.

## APPENDIX

## EQUILIBRIUM SPEED OF SOUND IN IONIZING ARGON

The equilibrium speed of sound in ionizing argon is calculated with the assumptions:

- (1) single degree of ionization
- (2) perfect-gas equations for argon atoms, ions, and electrons.

If  $\alpha$  denotes the degree of ionization, i. e., the mass fraction of argon ions, the equation of state of the mixture of atoms, ions and electrons may be written as

$$p = (1 + \alpha) \rho R T \quad (\text{A. 1})$$

where  $R$  is the gas constant of the argon atom, and the enthalpy is given by

$$\begin{aligned} h &= h_A + (2h_{A+} - h_A) \alpha \\ &= 5/2 RT - e_o + (5/2 RT + e_o) \alpha, \end{aligned} \quad (\text{A. 2})$$

where  $e_o$  is the heat of ionization per unit mass at  $0^\circ\text{K}$ . From the thermodynamic formulas, it can be shown that

$$a_e^2 = (\partial p / \partial \rho)_s = \frac{c_p}{c_p (\partial \rho / \partial p)_T - (T/\rho^2) (\partial \rho / \partial T)_p^2} \quad (\text{A. 3})$$

Calculating  $c_p$ ,  $(\partial \rho / \partial p)_T$  and  $(\partial \rho / \partial T)_p$  from Eqs. A. 1 and A. 2 and substituting in Eq. A. 3, we obtain, with  $a_o^2 = 5/3 \gamma p / \rho$ ,

$$\left(\frac{a_e}{a_o}\right)^2 = \frac{1 + \left(1 + \frac{2}{5} \frac{e_o}{RT}\right) \frac{T}{1+a} \left(\frac{\partial a}{\partial T}\right)_p}{1 - \frac{5}{3} \frac{p}{1+a} \left(\frac{\partial a}{\partial p}\right)_T + \frac{1}{3} \left(1 + 2 \frac{e_o}{RT}\right) \frac{T}{1+a} \left(\frac{\partial a}{\partial T}\right)_p - \frac{5}{3} \left[ \dots \right.} \quad (\text{A. 4})$$

$$\left. \dots \left(1 + \frac{2}{5} \frac{e_o}{RT}\right) \frac{p}{1+a} \left(\frac{\partial a}{\partial p}\right)_T - \frac{2}{5} \frac{T}{1+a} \left(\frac{\partial a}{\partial T}\right)_p \right] \frac{T}{1+a} \left(\frac{\partial a}{\partial T}\right)_p} .$$

Applying the law of mass action to the ionization of argon, we obtain

$$\frac{a^2}{1-a^2} = \frac{K(T)}{p} . \quad (\text{A. 5})$$

From the reciprocity relations of thermodynamics we have

$$(\partial h / \partial p)_T = v - T (\partial v / \partial T)_p . \quad (\text{A. 5})$$

From Eq. A. 2, we obtain the relation

$$(\partial h / \partial p)_T = \ell_I (\partial a / \partial p)_T , \quad (\text{A. 7})$$

where  $\ell_I = 2h_{A_+} - h_A$  .

From Eqs. A. 1, A. 6, and A. 7, we obtain

$$\ell_I (\partial a / \partial p)_T = - \frac{R_3 T^2}{p} (\partial a / \partial T)_p . \quad (\text{A. 8})$$

Computing  $(\partial a / \partial p)_T$  and  $(\partial a / \partial T)_p$  from Eq. A. 5, substituting in Eq. A. 8, yields

$$\frac{1}{K} \frac{dK}{dt} = \frac{\ell_I}{RT^2} = \frac{5}{2} \frac{1}{T} + \frac{e_o}{RT^2} ,$$

and

$$K = \text{constant} \cdot T^{5/2} \exp \left( - \frac{e_o}{RT} \right) .$$

Hence, we obtain

$$\begin{aligned} (\partial a / \partial T)_P &= \left( 5/2 + \frac{e_o}{RT} \right) \frac{a(1-a)^2}{2T} \\ (\partial a / \partial P)_T &= - \frac{(1-a)^2}{2P} a \end{aligned} \quad (A.9)$$

which, introduced in Eq. A.4, give

$$\left( \frac{a_e}{a_o} \right)^2 = \frac{\theta^2 + \frac{5}{4} \left( \frac{2}{5} + \theta \right)^2 a (1-a)}{\theta^2 + \frac{5}{12} \left[ 2\theta^2 + \left( \theta + \frac{2}{5} \right) (\theta + 2) \right] a(1-a) + \frac{25}{12} \left( \theta + \frac{2}{5} \right)^2 a^2 (1-a)^2} \quad (A.10)$$

where  $\theta = (T/\theta_i)$  and  $\theta_i \equiv (e_o/R) = 182.9 \times 10^3$  °K for argon.

In Eq. A.10,  $\theta$  being very small,  $a$  small, terms of order  $\theta^2 a$  can be neglected. Finally:

$$\left( \frac{a_e}{a_o} \right)^2 = \frac{\theta^2 + \frac{1}{5} (1 + 5\theta) a (1-a)}{\theta^2 + \frac{1}{3} (1 + 3\theta) a (1-a) + \frac{1}{3} (1 + 5\theta) a^2 (1-a)^2} \quad (A.11)$$



TABLE 1

## GAS PROPERTIES AT SONIC CONDITION

Remarks: (1)  $a_e$  computed by the formulas of the Appendix  
 (2)  $a_e$  neglected under  $10^{-3}$

Reference: Mollier Chart for Argon<sup>2</sup>

1.  $p_t = 1 \text{ atm}$

|                                                     | Point        | 1                  | 2                  | 3                  | 4                | 5                | 6                  | 7                  | 8                  | 9                  |
|-----------------------------------------------------|--------------|--------------------|--------------------|--------------------|------------------|------------------|--------------------|--------------------|--------------------|--------------------|
| Dim.                                                | Quant.       |                    |                    |                    |                  |                  |                    |                    |                    |                    |
| $^{\circ}\text{K}$                                  | $T_t$        | 14,000             | 12,000             | 11,000             | 10,000           | 8,000            | 6,000              | 5,000              | 4,000              | 3,000              |
| -                                                   | $a_t$        | 0.4                | 0.115              | 0.053              | 0.022            | 0.0015           | $\sim 0$           | $\sim 0$           | $\sim 0$           | $\sim 0$           |
| -                                                   | $h_t/RT_o$   | 445                | 199                | 141                | 107              | 74               | 54                 | 45                 | 37                 | 27                 |
| $\frac{\text{m}}{\text{sec}}$                       | $v^*=a_e^*$  | 1,885              | 1,670              | 1,605              | 1,590            | 1,470            | 1,250              | 1,140              | 1,020              | 883                |
| -                                                   | $h^*/RT_o$   | 414                | 174.6              | 118.4              | 84.7             | 55               | 54                 | 45                 | 37                 | 27                 |
| $\frac{\text{n}}{\text{m}^2}$                       | $p^*$        | $59.7 \times 10^3$ | $59.6 \times 10^3$ | $54.5 \times 10^3$ | $52 \times 10^3$ | $47 \times 10^3$ | $49.4 \times 10^3$ | $49.4 \times 10^3$ | $49.4 \times 10^3$ | $49.4 \times 10^3$ |
| $^{\circ}\text{K}$                                  | $T^*$        | 13,460             | 11,340             | 10,180             | 8,680            | 6,100            | 4,500              | 3,750              | 3,000              | 2,250              |
| -                                                   | $a^*$        | 0.37               | 0.0906             | 0.0328             | 0.0049           | $\sim 0$         | $\sim 0$           | $\sim 0$           | $\sim 0$           | $\sim 0$           |
| $\frac{\text{kgmass}}{\text{m}^3}$                  | $\rho^*$     | 0.01553            | 0.0231             | 0.0249             | 0.0286           | 0.037            | 0.0527             | 0.0633             | 0.0790             | 0.0820             |
| $\frac{\text{kgmass}}{\text{m}^2 \cdot \text{sec}}$ | $\rho^* a^*$ | 29.3               | 38.6               | 40.0               | 45.5             | 54.3             | 65.9               | 72.2               | 80.6               | 93                 |

TABLE 1 (CONTINUED)

2.  $p_t = 2 \text{ atm}$ 

|                                                     | Point        | 1                 | 2                   | 3      | 4        | 5                  | 6                  | 7                  |
|-----------------------------------------------------|--------------|-------------------|---------------------|--------|----------|--------------------|--------------------|--------------------|
| Dim.                                                | Quant.       |                   |                     |        |          |                    |                    |                    |
| $^{\circ}\text{K}$                                  | $T_t$        | 14,000            | 12,000              | 11,000 | 9,000    | 6,000              | 5,000              | 4,000              |
| -                                                   | $a_t$        | 0.2918            | 0.082               | 0.037  | 0.033    | $\sim 0$           | $\sim 0$           | $\sim 0$           |
| -                                                   | $h_t/RT_o$   | 358               | 175                 | 129    | 86       | 54                 | 45                 | 37                 |
| $\frac{\text{m}}{\text{sec}}$                       | $v^*=a_e^*$  | 1,828             | 1,680               | 1,682  | 1,535    | 1,250              | 1,140              | 1,020              |
| -                                                   | $h-/RT_o$    | 328.6             | 150.4               | 104    | 64.5     | 54                 | 45                 | 37                 |
| $\frac{n}{\text{m}^2}$                              | $p^*$        | $130 \times 10^3$ | $117.2 \times 10^3$ | 104    | 102      | $98.8 \times 10^3$ | $98.8 \times 10^3$ | $98.8 \times 10^3$ |
| $^{\circ}\text{K}$                                  | $T^*$        | 13,405            | 11,290              | 9,880  | 7,050    | 4,500              | 3,750              | 3,000              |
| -                                                   | $a^*$        | 0.2675            | 0.0609              | 0.0184 | $\sim 0$ | $\sim 0$           | $\sim 0$           | $\sim 0$           |
| $\frac{\text{kgmass}}{\text{m}^3}$                  | $\rho^*$     | 0.03672           | 0.047               | 0.0497 | 0.0695   | 0.1054             | 0.1266             | 0.158              |
| $\frac{\text{kgmass}}{\text{m}^2 \cdot \text{sec}}$ | $\rho^* a^*$ | 67.1              | 78.5                | 84.0   | 108.7    | 131.8              | 144.4              | 161.2              |

TABLE 2

## SUMMARY OF PRELIMINARY EXPERIMENTS

Remark: In connection with Section 4, it is mentioned that the tests described below correspond to a geometry:  $d'$  (Figure 10) = 0.43";  $\phi = \frac{1}{2}"$ ;  $l/\phi = 3.14$

Pressure in chamber: 1 atm  $\sim$  0.2 psi

| Test | Injection Angle | Electrodes | Electrode Distance* (in) | $V_{arc}$ ; Variation with d           | Gas Mass Flow (gr/sec) | Power Input (max.) | Efficiency | $V_{arc}$ (volts) | $I_{arc}$ (amp) | Remarks                                          |
|------|-----------------|------------|--------------------------|----------------------------------------|------------------------|--------------------|------------|-------------------|-----------------|--------------------------------------------------|
| A-7  | $90^\circ$      | > +        | 1-7/8                    | Insensitive to d, except for stability | 1.4                    | 4 kw               | 50~70%     | 45~50             | 70~130          | Electrodes copper - copper; arc fairly stable    |
| S-1  | $90^\circ$      | > -        | 1-3/4 2                  | Increases slightly with d              | 1.4                    | 2.4 kw             | --         | 50~60             | 25~60           | Electrodes copper - copper arc unstable          |
| S-11 | $90^\circ$      | > +        | 2                        | <u>Figure 11 and 13</u>                | 0.92~1.98              | 8 kw               | 42~72      | 33~46             | 50~180          | Electrodes: >+ copper; >-thoriated tungsten ring |
| S-22 | $0^\circ$       | > +        | 2                        | 11 and 13                              | 0.92~1.98              | 8 kw               | 30~68      | 36~46             | 50~170          | Electrodes: see S-11                             |
| S-26 | $0^\circ$       | > +        | 2                        | 11 and 13                              | 0.92~1.98              | 8 kw               | 55~75      | 35~48             | 40~180          | Electrodes: see S-11                             |

\* From tip of central electrode to exit section

TABLE 2 (CONTINUED)

| Test | Injection Angle | Elec- trodes | Electrode Distance* (in) | Figure    | Gas Mass Flow(gr/sec) | Power Input (max.) | Efficiency | V <sub>arc</sub> (volts) | I <sub>arc</sub> (amp) | Remarks                                                          |
|------|-----------------|--------------|--------------------------|-----------|-----------------------|--------------------|------------|--------------------------|------------------------|------------------------------------------------------------------|
| O-11 | 90°             | > -          | 1.57                     | 12 and 13 | 0.92~1.98             | 4.5 kw             | 35~45      | 22~26                    | 40~190                 | Electrodes: >+ with tungsten tip (Fig. 9), >- with tungsten tube |
| O-12 | 45°             | > -          | 1.57                     | 12 and 13 | 0.92~1.98             | 4.5 kw             | 37~50      | 22~26                    | 40~190                 | Electrodes: See O-11                                             |

\* From tip of central electrode to exit section

TABLE 3

## EXPERIMENTS PERFORMED

|                 |              | Values of $\dot{M}_0$ (gr/sec x inches <sup>2</sup> ) |                   |                  |                    |                  |                  |                  |
|-----------------|--------------|-------------------------------------------------------|-------------------|------------------|--------------------|------------------|------------------|------------------|
| $m'$ (gr/sec)   |              | 6.00                                                  | 4.24              | 3.00             | 2.12               | 1.50             | 1.06             |                  |
| $\phi$ (inches) |              |                                                       |                   |                  |                    |                  |                  |                  |
| 1/2             | $l/\phi = 8$ | > +                                                   | 30.56<br>N-22, I  | 21.6<br>N-22, II | 15.28<br>N-22, III | 10.8<br>O-27, I  | 7.64<br>O-27, II | 5.4<br>O-27, III |
|                 |              | > -                                                   | 30.56<br>N-22, IV | 21.6<br>N-22, V  | 15.28<br>N-22, VI  | 10.8<br>O-27, IV | 7.64<br>O-27, V  | 5.4<br>O-27, VI  |
|                 | $l/\phi = 4$ | > +                                                   |                   |                  |                    | 10.8<br>O-25, I  | 7.64<br>O-25, II | 5.4<br>O-25, III |
|                 |              | > -                                                   |                   |                  |                    | 10.8<br>O-25, IV | 7.64<br>O-25, V  | 5.4<br>O-25, VI  |
|                 | $l/\phi = 2$ | > +                                                   | 30.56<br>N-26, I  | 21.6<br>N-26, II | 15.28<br>N-26, III | 10.8<br>O-20, I  | 7.64<br>O-20, II | 5.4<br>O-20, III |
|                 |              | > -                                                   | 30.56<br>N-26, IV | 21.6<br>N-26, V  | 15.28<br>N-26, VII | 10.8<br>O-20, IV | 7.64<br>O-20, V  | 5.4<br>O-20, VI  |
|                 | $l/\phi = 1$ | > +                                                   |                   |                  |                    | 10.8<br>O-29, I  | 7.64<br>O-29, II | 5.4<br>O-29, III |
|                 |              | > -                                                   |                   |                  |                    | 10.8<br>O-29, IV | 7.64<br>O-29, V  | 5.4<br>O-29, VI  |



TABLE 3 (CONTINUED)

|                 |              | Values of $\mathcal{H}$ (gr/sec x inches <sup>2</sup> ) |                   |                  |                    |                  |                   |                   |
|-----------------|--------------|---------------------------------------------------------|-------------------|------------------|--------------------|------------------|-------------------|-------------------|
| $m'$ (gr/sec)   |              | 6.00                                                    | 4.24              | 3.00             | 2.12               | 1.50             | 1.06              |                   |
| $\phi$ (inches) |              |                                                         |                   |                  |                    |                  |                   |                   |
| 0.354           | $l/\phi = 8$ | > +                                                     | 61.12<br>N-20, I  | 43.2<br>N-20, II | 30.56<br>N-20, III | 21.6<br>N-7, I   | 15.28<br>N-7, II  | 10.8<br>N-7, III  |
|                 |              | > -                                                     | 61.12<br>N-20, IV | 43.2<br>N-20, V  | 30.56<br>N-20, VI  | 21.6<br>N-7, IV  | 15.28<br>N-7, V   | 10.8<br>N-7, VI   |
|                 | $l/\phi = 4$ | > +                                                     |                   |                  |                    | 21.6<br>N-8, I   | 15.28<br>N-8, II  | 10.8<br>N-8, III  |
|                 |              | > -                                                     |                   |                  |                    | 21.6<br>N-8, IV  | 15.28<br>N-8, V   | 10.8<br>N-8, VI   |
|                 | $l/\phi = 2$ | > +                                                     | 61.12<br>N-21, I  | 43.2<br>N-21, II | 30.56<br>N-21, III | 21.6<br>N-9, I   | 15.28<br>N-9, II  | 10.8<br>N-9, III  |
|                 |              | > -                                                     | 61.12<br>N-21, IV | 43.2<br>N-21, V  | 30.56<br>N-21, VI  | 21.6<br>N-9, IV  | 15.28<br>N-9, V   | 10.8<br>N-9, VI   |
|                 | $l/\phi = 1$ | > +                                                     |                   |                  |                    | 21.6<br>N-10, I  | 15.28<br>N-10, II | 10.8<br>N-10, III |
|                 |              | > -                                                     |                   |                  |                    | 21.6<br>N-10, IV | 15.28<br>N-10, V  | 10.8<br>N-10, VI  |

TABLE 3 (CONTINUED)

|                 |              | Values of $\mathcal{H}_C$ (gr/sec x inches <sup>2</sup> ) |                    |                  |                    |                  |                   |                   |
|-----------------|--------------|-----------------------------------------------------------|--------------------|------------------|--------------------|------------------|-------------------|-------------------|
| $m'$ (gr/sec)   |              | 6.00                                                      | 4.24               | 3.00             | 2.12               | 1.50             | 1.06              |                   |
| $\phi$ (inches) |              |                                                           |                    |                  |                    |                  |                   |                   |
| 1/4             | $l/\phi = 8$ | > +                                                       | 122.24<br>N-19, I  | 86.4<br>N-19, II | 61.12<br>N-19, III | 43.2<br>N-11, I  | 30.56<br>N-11, II | 21.6<br>N-11, III |
|                 |              | > -                                                       | 122.24<br>N-19, IV | 86.4<br>N-19, V  | 61.12<br>N-19, VI  | 43.2<br>N-11, IV | 30.56<br>N-11, V  | 21.6<br>N-11, VI  |
|                 | $l/\phi = 4$ | > +                                                       |                    |                  |                    | 43.2<br>N-2, I   | 30.56<br>N-2, II  | 21.6<br>N-2, III  |
|                 |              | > -                                                       |                    |                  |                    | 43.2<br>N-2, IV  | 30.56<br>N-2, V   | 21.6<br>N-2, VI   |
|                 | $l/\phi = 2$ | > +                                                       | 122.24<br>N-18, I  | 86.4<br>N-18, II | 61.12<br>N-18, III | 43.2<br>N-14, I  | 30.56<br>N-14, II | 21.6<br>N-14, III |
|                 |              | > -                                                       | 122.24<br>N-18, IV | 86.4<br>N-18, V  | 61.12<br>N-18, VI  | 43.2<br>N-14, IV | 30.56<br>N-14, V  | 21.6<br>N-14, VI  |
|                 | $l/\phi = 1$ | > +                                                       |                    |                  |                    | 43.2<br>N-15, I  | 30.56<br>N-15, II | 21.6<br>N-15, III |
|                 |              | > -                                                       |                    |                  |                    | 43.2<br>N-15, IV | 30.56<br>N-15, V  | 21.6<br>N-15, VI  |

TABLE 4

## EXPERIMENTS OF SYSTEMATIC STUDY

Variation of efficiency and voltage drop across the arc with the independent variables

1. Optimum choice of variables for best  $\eta$ ,  $V_{\text{arc}}$ ,  $\bar{T}_g$

(a) Polarities: For best  $\eta$ ,  $V_{\text{arc}}$ ,  $\bar{T}_g$ , > + has to be preferred to > -

(b) Whatever the polarity:

For best

One must take

|                  | Polarity | $\mathcal{M}$ | $l/\phi$ | $\phi$                                          | $m'$  | Injection Angle |
|------------------|----------|---------------|----------|-------------------------------------------------|-------|-----------------|
| $\eta$           | > +      | large         | large    | small                                           | large | $45^\circ$      |
|                  | > -      | large         | small    | unimportant at small $m'$ ; small at large $m'$ | large | $45^\circ$      |
| $V_{\text{arc}}$ | > +      | large         | large    | small                                           | large | $45^\circ$      |
|                  | > -      | large         | small    | unimportant at small $m'$ ; small at large $m'$ |       | $45^\circ$      |

$\bar{T}_g$  Since  $\bar{T}_g$  increases with  $\frac{\eta P_{\text{input}}}{m'}$ , i. e., increases with decreasing  $\phi$  and decreasing mass flow, the "mass factor"  $\mathcal{M}$ , ratio of two small quantities, takes an "intermediate" value for optimum  $\bar{T}_g$ . The maximum temperatures ( $\approx 10,000^\circ\text{K}$ ) were obtained for  $\mathcal{M} = 20$  to 30 (gr/sec. inches<sup>2</sup>)

TABLE 4 (CONTINUED)

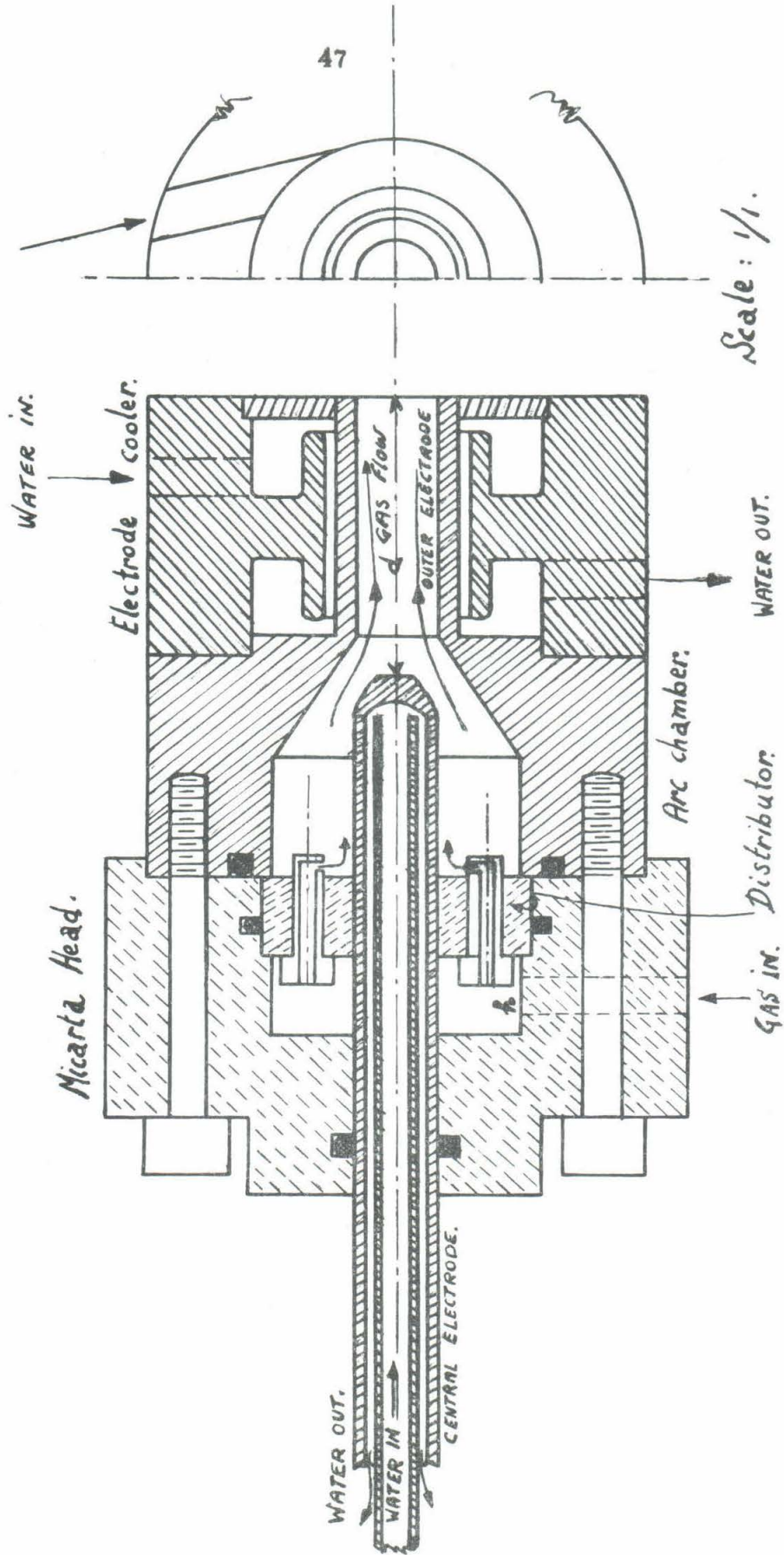
| 2. Variation of Efficiency                                           |               |                                             |                             |
|----------------------------------------------------------------------|---------------|---------------------------------------------|-----------------------------|
| Fixed Quantities                                                     | Polarity Case | Variation of Efficiency                     | Independent Variable        |
| power input, geometry, mass flow                                     | --            | $\eta_{>+} > \eta_{>-}$                     | polarity                    |
| polarity, geometry, mass flow                                        | all           | $\eta \searrow$                             | $P_{\text{input}} \nearrow$ |
| polarity, mass flow, power input and $\phi$ fixed, $l/\phi$ variable | $>+$          | $\eta \nearrow$                             | $l/\phi \nearrow$           |
|                                                                      | $>-$          | $\eta \searrow$                             | $l/\phi \nearrow$           |
| $l/\phi$ fixed, $\phi$ variable                                      | $>+$          | $\eta \searrow$                             | $\phi \nearrow$             |
|                                                                      | $>-$          | small mass flows:<br>practically unaffected | $\phi \nearrow$             |
|                                                                      |               | -----                                       |                             |
|                                                                      |               | large mass flows:<br>$\eta \searrow$        | $\phi \nearrow$             |
| polarity, geometry, power input                                      | all           | $\eta \nearrow$                             | $m' \nearrow$               |
| polarity, $l/\phi$ , power input                                     | all           | $\eta \nearrow$                             | $HE \nearrow$               |

TABLE 4 (CONTINUED)

## 3. Variation of Voltage Drop Across the Arc

| Fixed Quantities                | Polarity Case | Variation of $V_{\text{arc}}$                               | Independent Variable        |
|---------------------------------|---------------|-------------------------------------------------------------|-----------------------------|
| polarity, geometry, mass flow   | > +           | $V_{\text{arc}} \nearrow$                                   | $P_{\text{input}} \nearrow$ |
| polarity, geometry, power input | all           | $V_{\text{arc}} \nearrow$                                   | $m' \nearrow$               |
| polarity, mass flow, current    |               |                                                             |                             |
| $\phi$ fixed, $l/\phi$ variable | > +           | $V_{\text{arc}} \nearrow$                                   | $l/\phi \nearrow$           |
|                                 | > -           | $V_{\text{arc}} \approx \text{constant}$                    | $l/\phi \nearrow$           |
| $l/\phi$ fixed, $\phi$ variable | > +           | $V_{\text{arc}} \searrow$                                   | $\phi \nearrow$             |
|                                 | > -           | $V_{\text{arc}} \nearrow$<br>slightly<br>at small mass flow | $\phi \nearrow$             |
|                                 |               | $V_{\text{arc}} \searrow$<br>at large mass flow             |                             |
| polarity, $l/\phi$ , current    |               | $V_{\text{arc}} \nearrow$<br>(strongly)                     | $HE \nearrow$               |





Scale: 1/1.

Fig. 1 Arc heater.

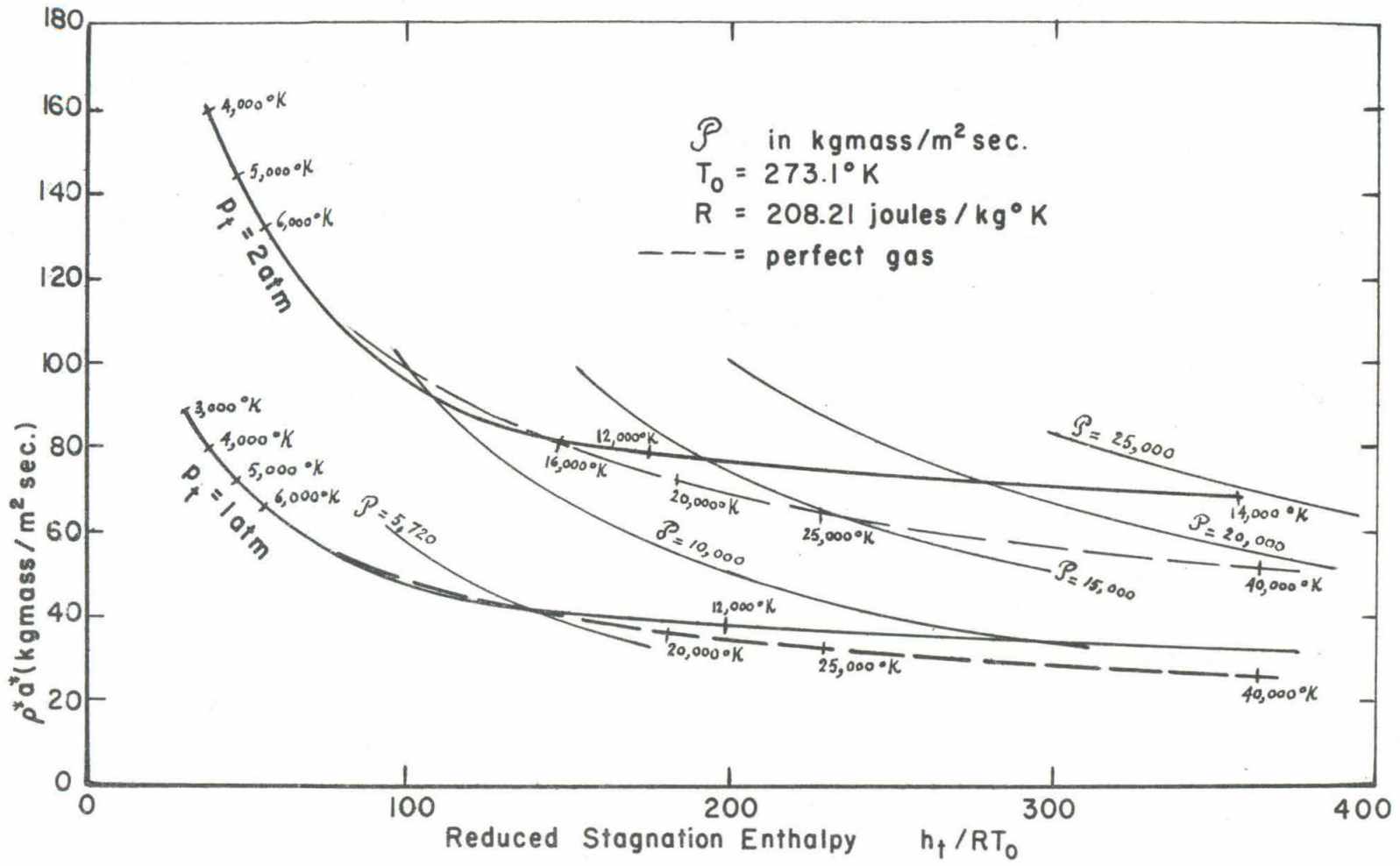
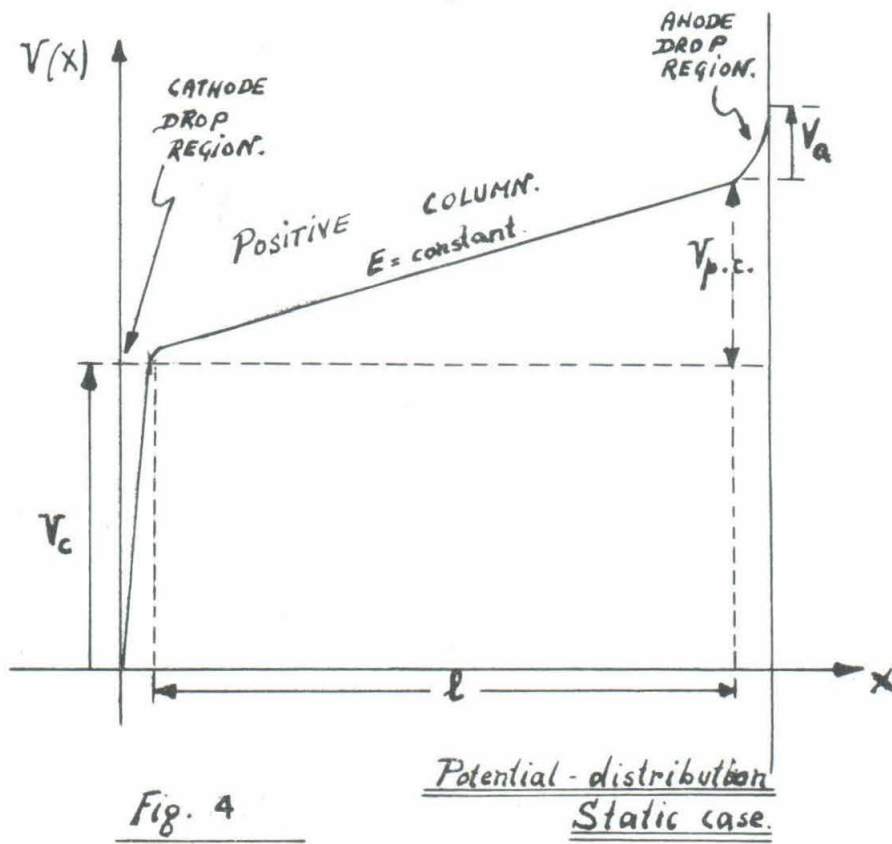
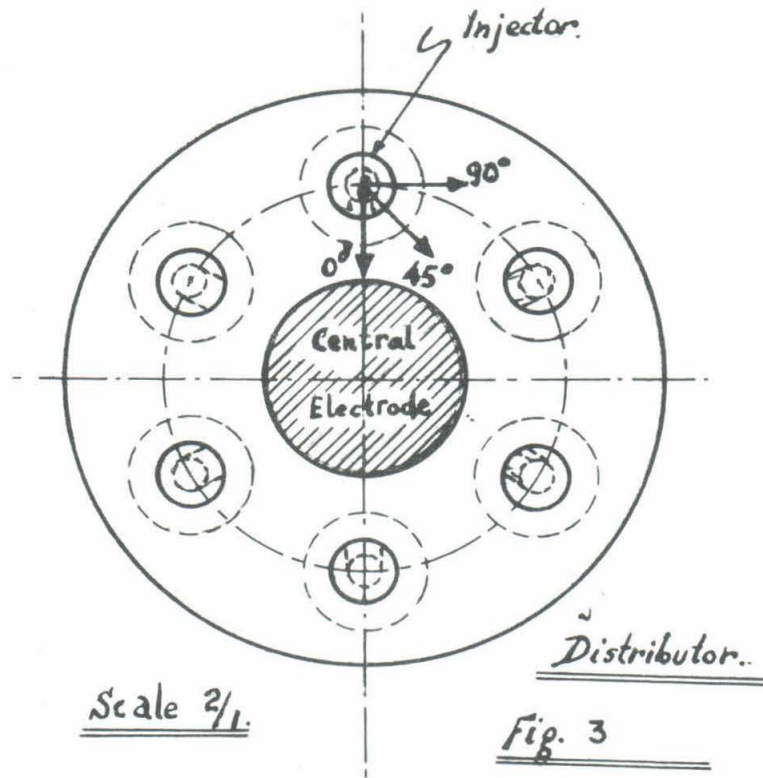
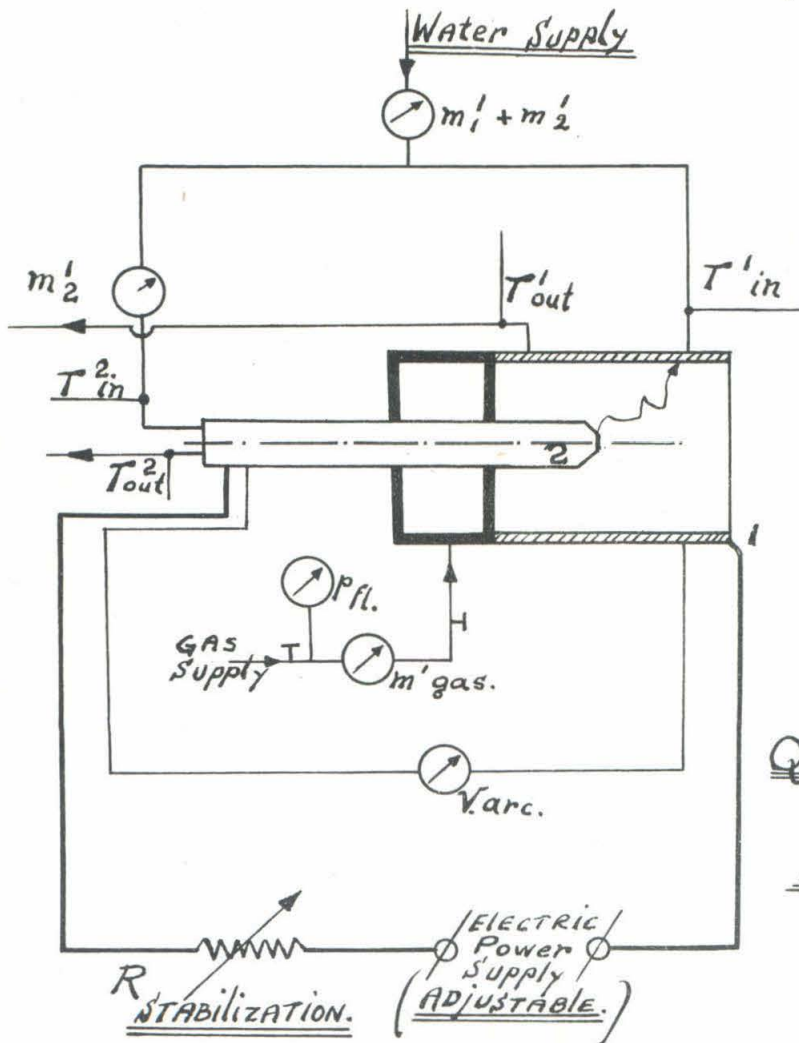
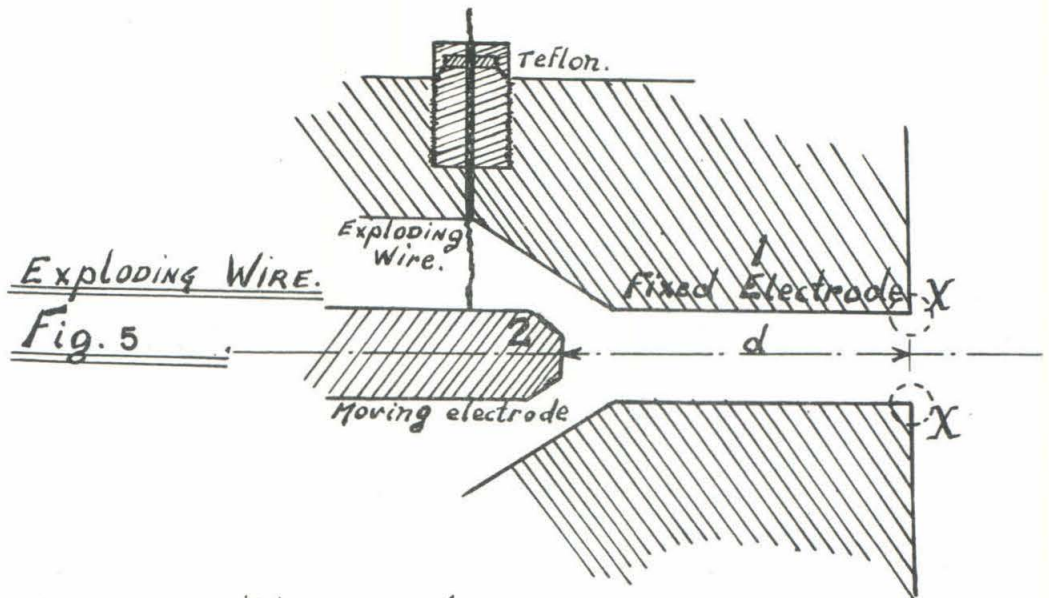


FIG. 2 CURVES  $\rho^* a^* = f\left(\frac{h_t}{RT_0}\right)$  and  $\mathcal{P} = \text{CONSTANT}$





Quantities  
measured.

Fig. 6

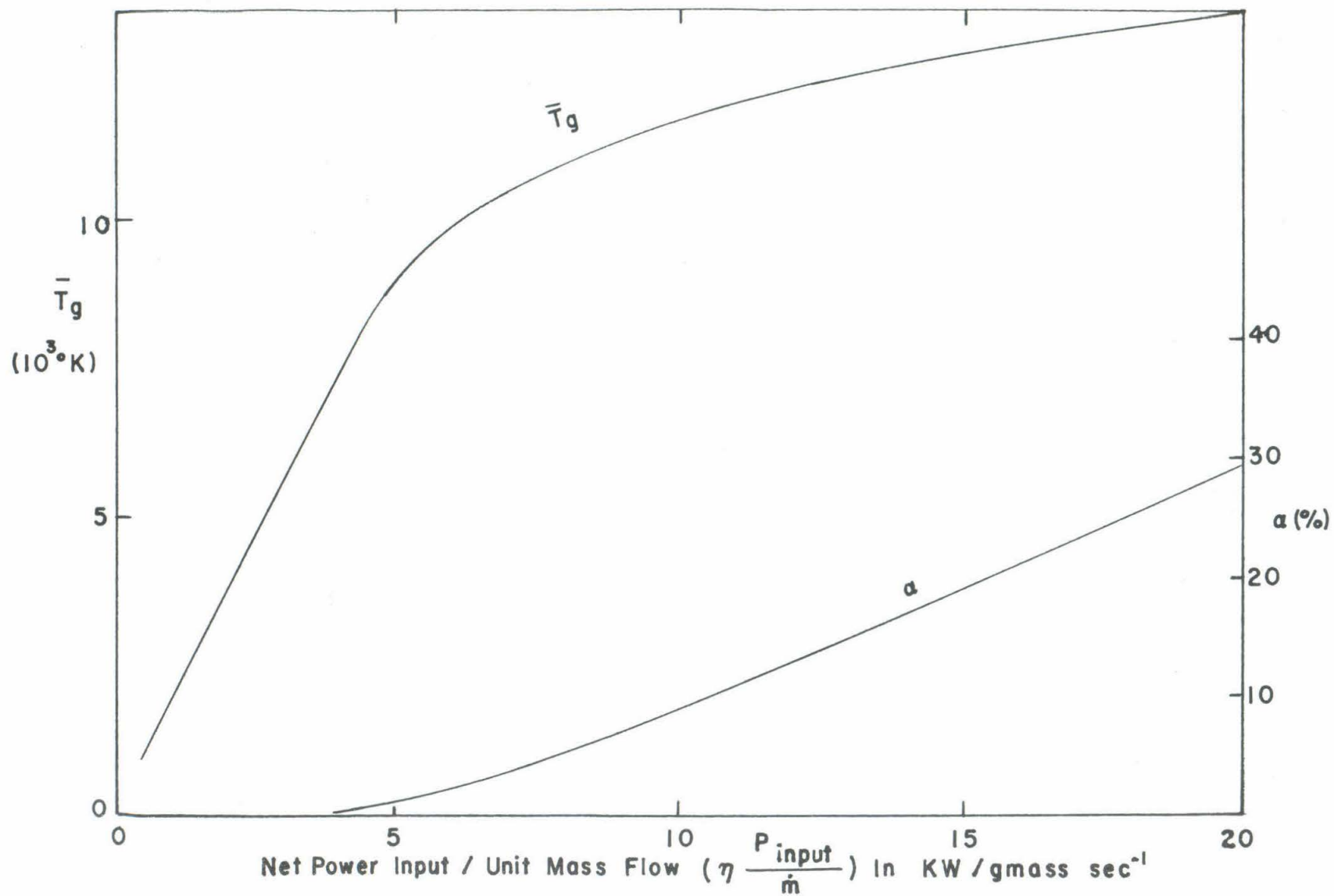


FIG. 7 ARGON AT P = 1 ATM.



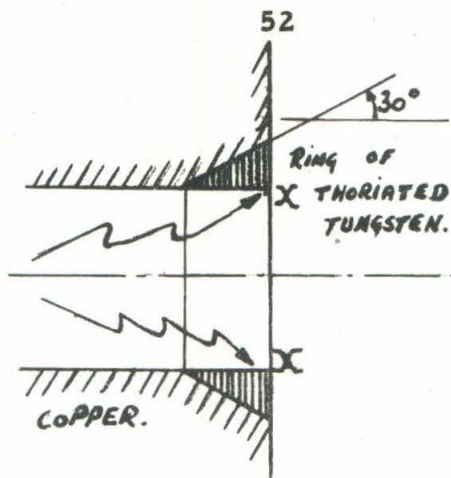
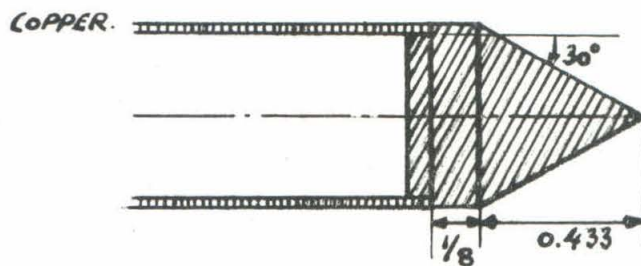


Fig. 8

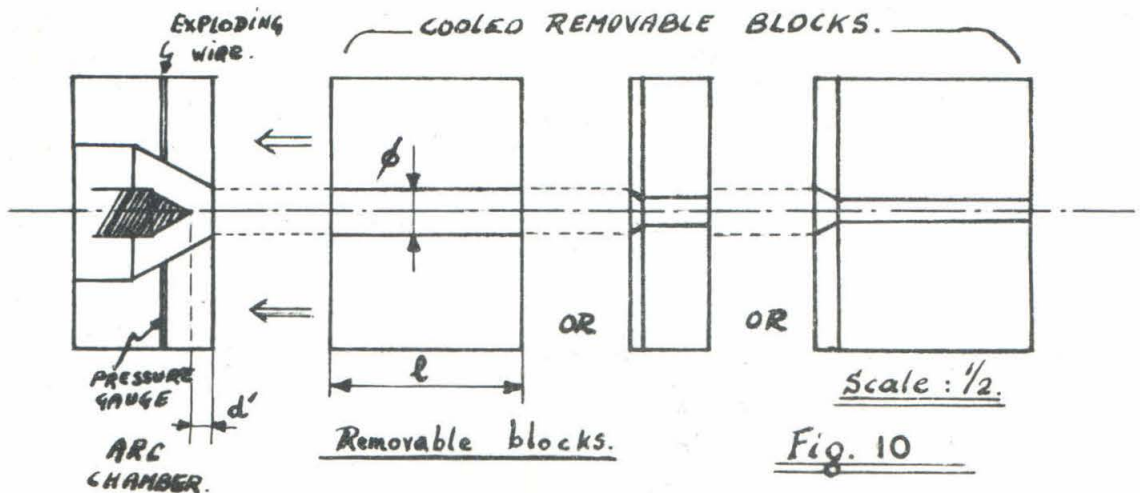
Sharp edge XX.

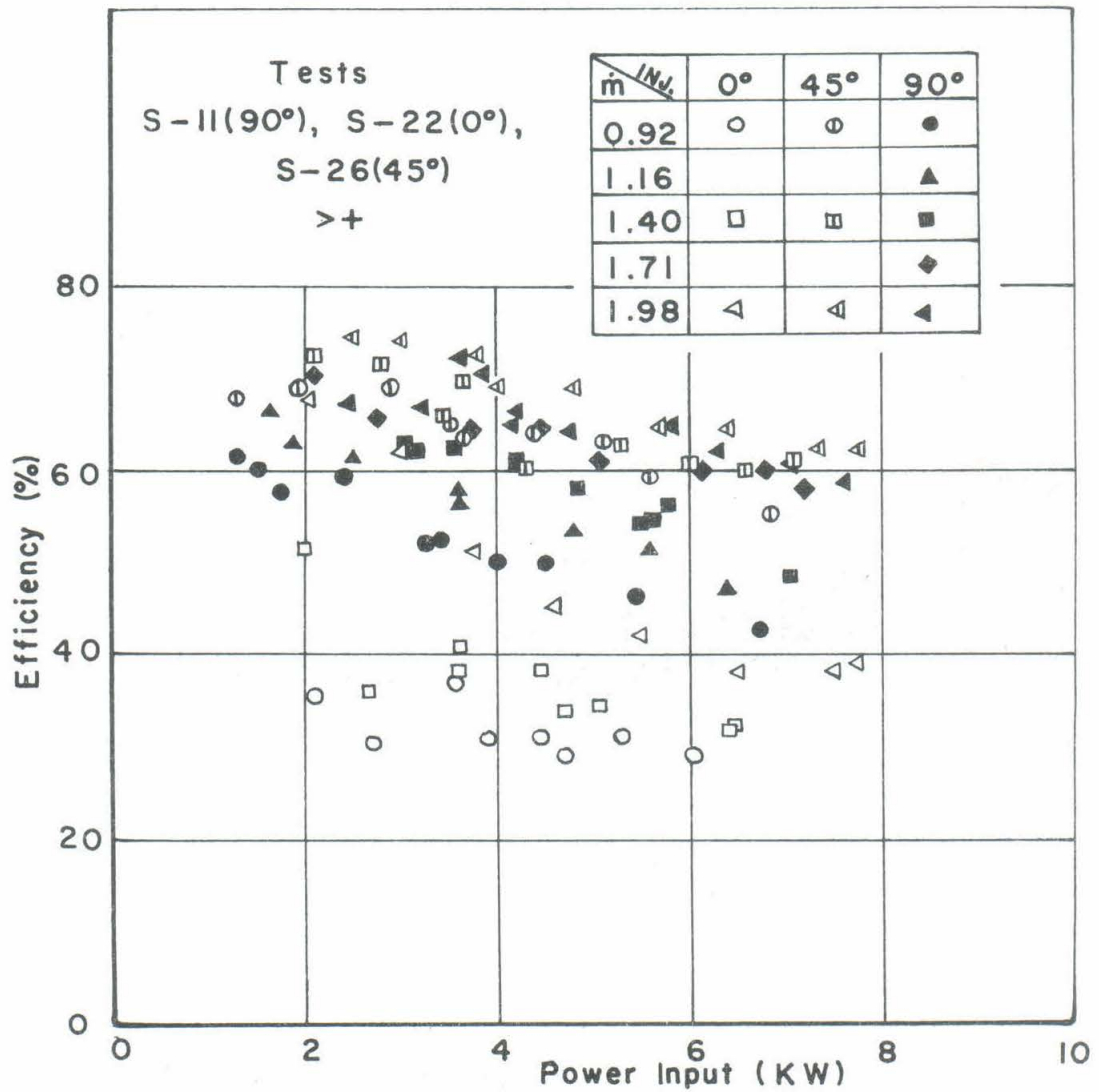


Scale  $\frac{2}{1}$ .

Thoriated Tungsten tip.

Fig. 9



FIG. II EFFICIENCY  $\eta$  VS. GROSS POWER INPUT

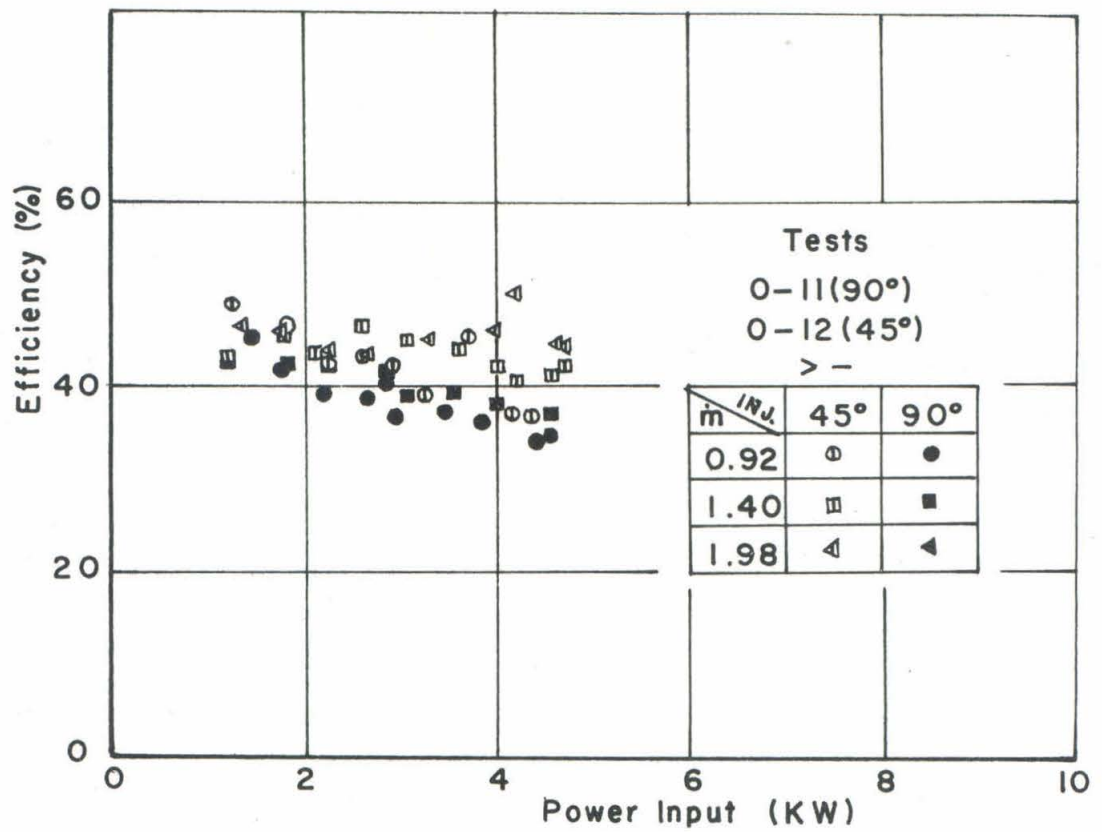


FIG. 12 EFFICIENCY  $\eta$  VS. GROSS POWER INPUT

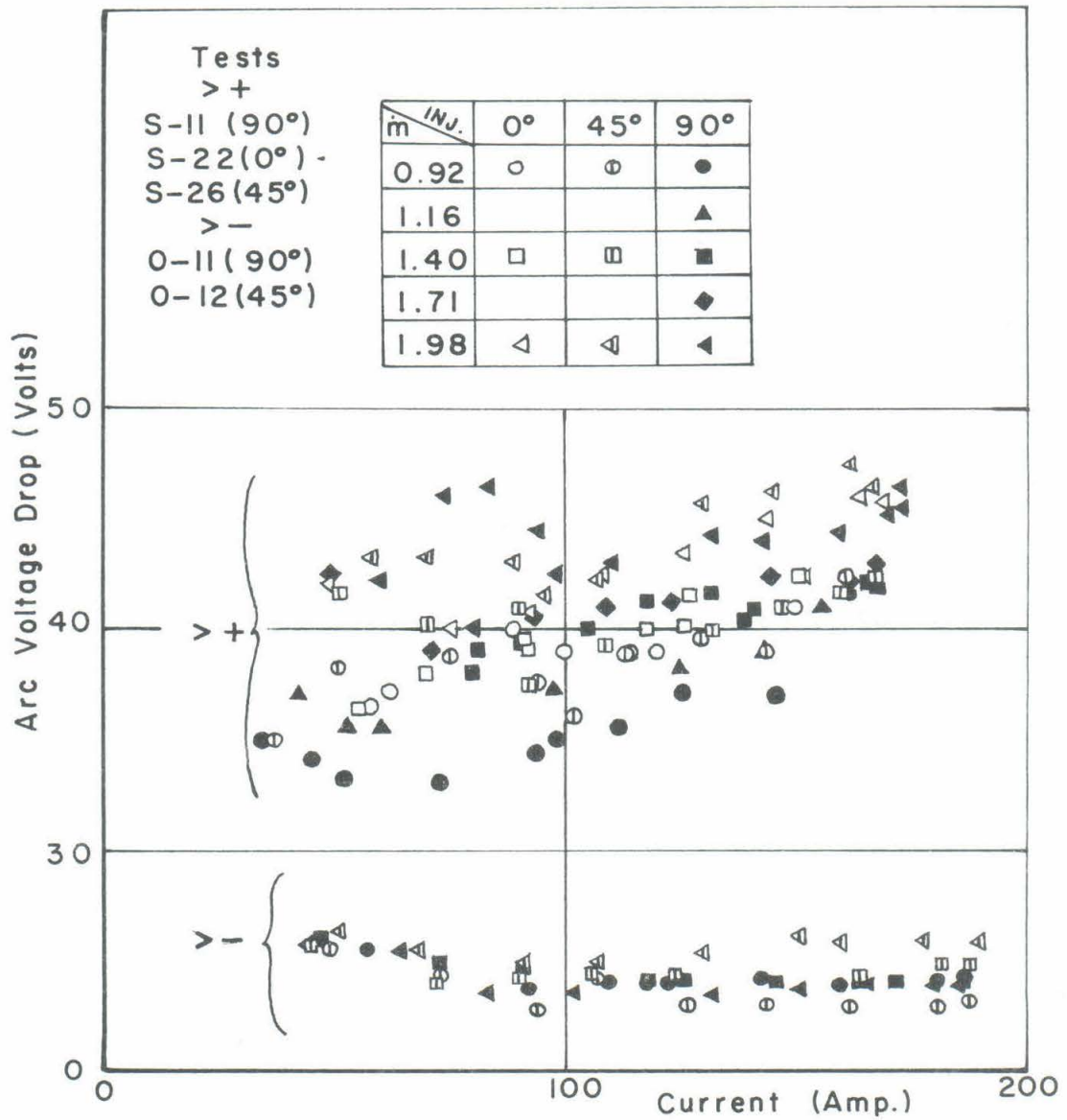


FIG. 13 ARC VOLTAGE DROP VS. CURRENT

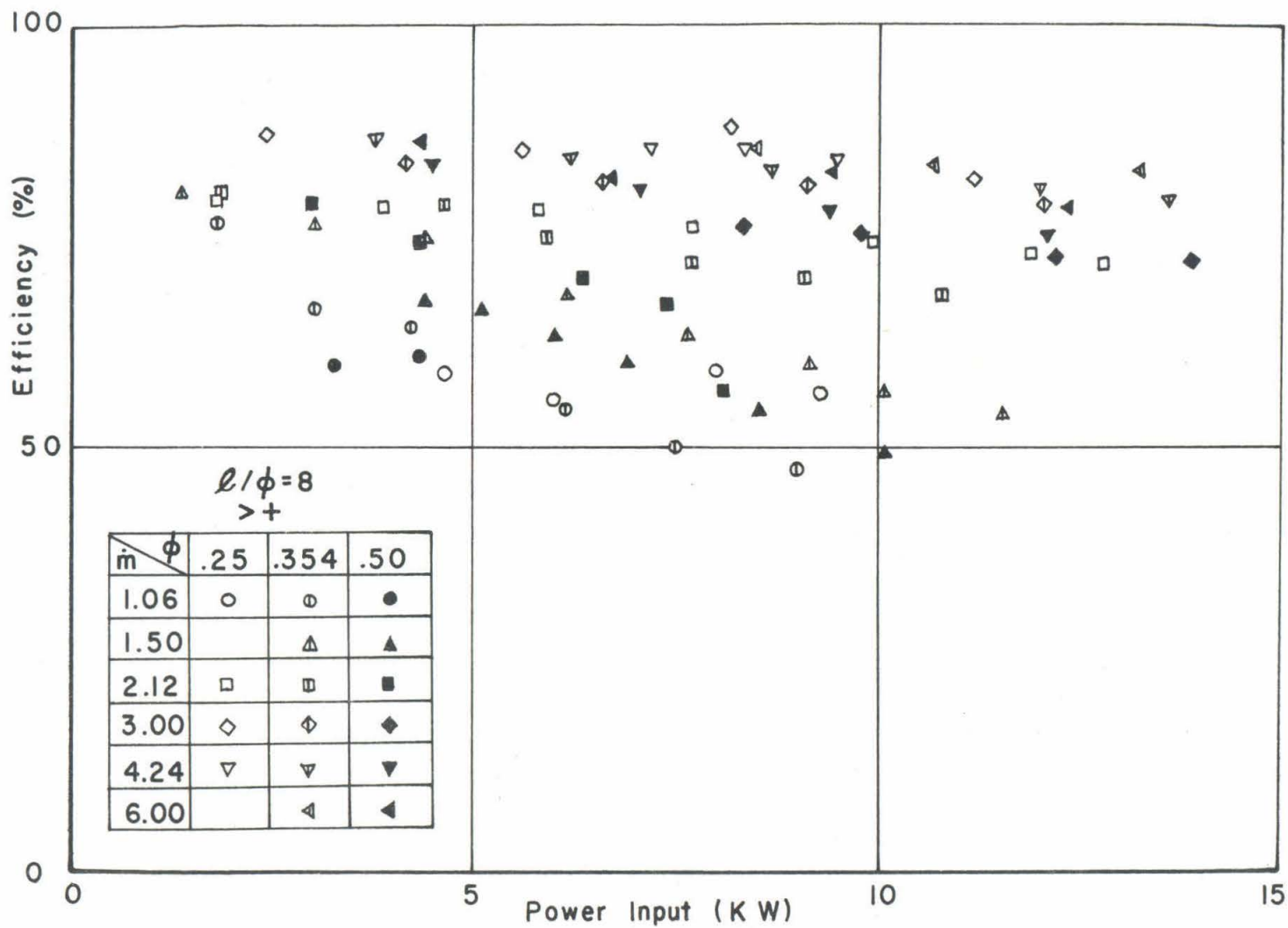


FIG.14 EFFICIENCY  $\eta$  VS. GROSS POWER INPUT



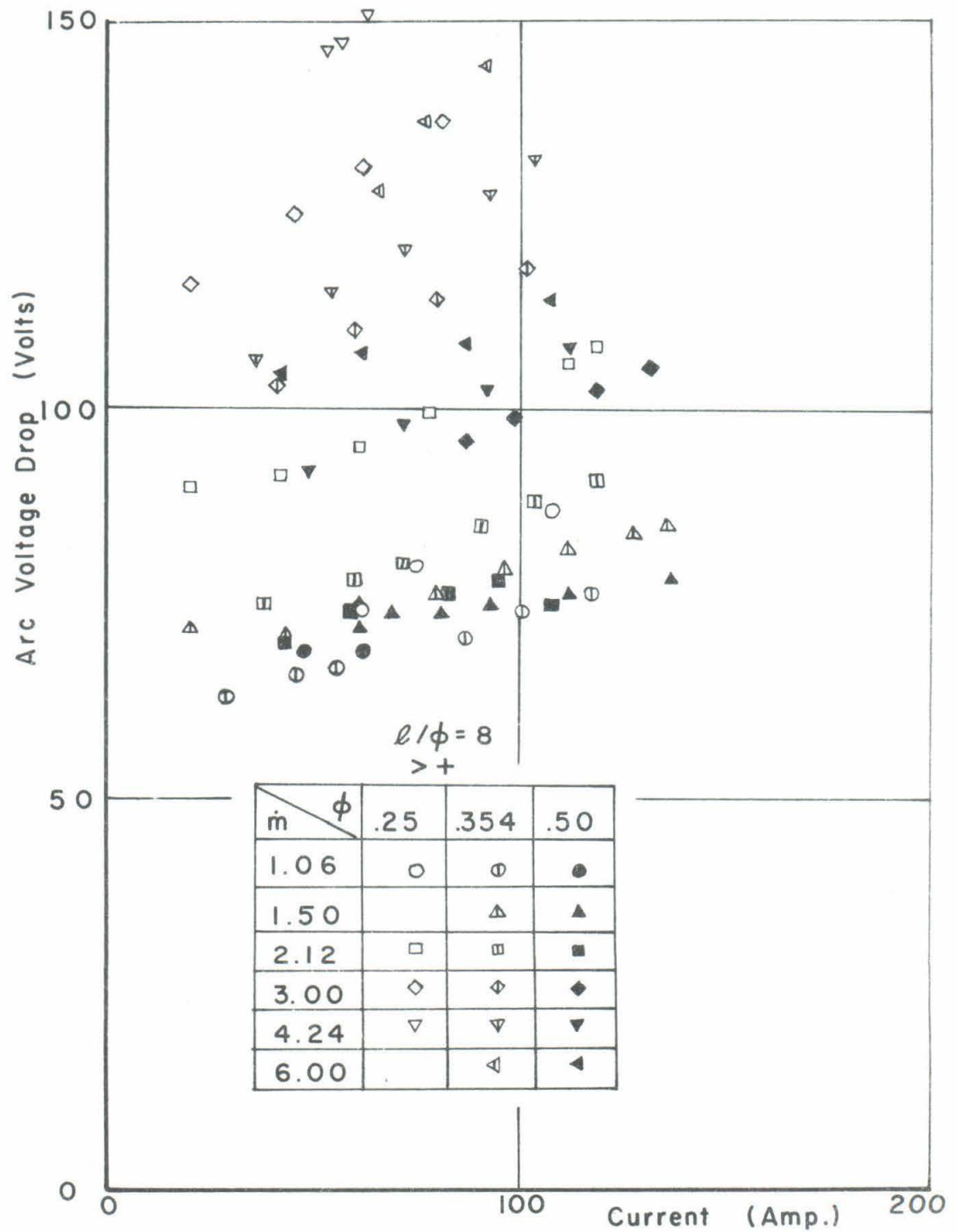


FIG. 15 ARC VOLTAGE DROP VS. CURRENT

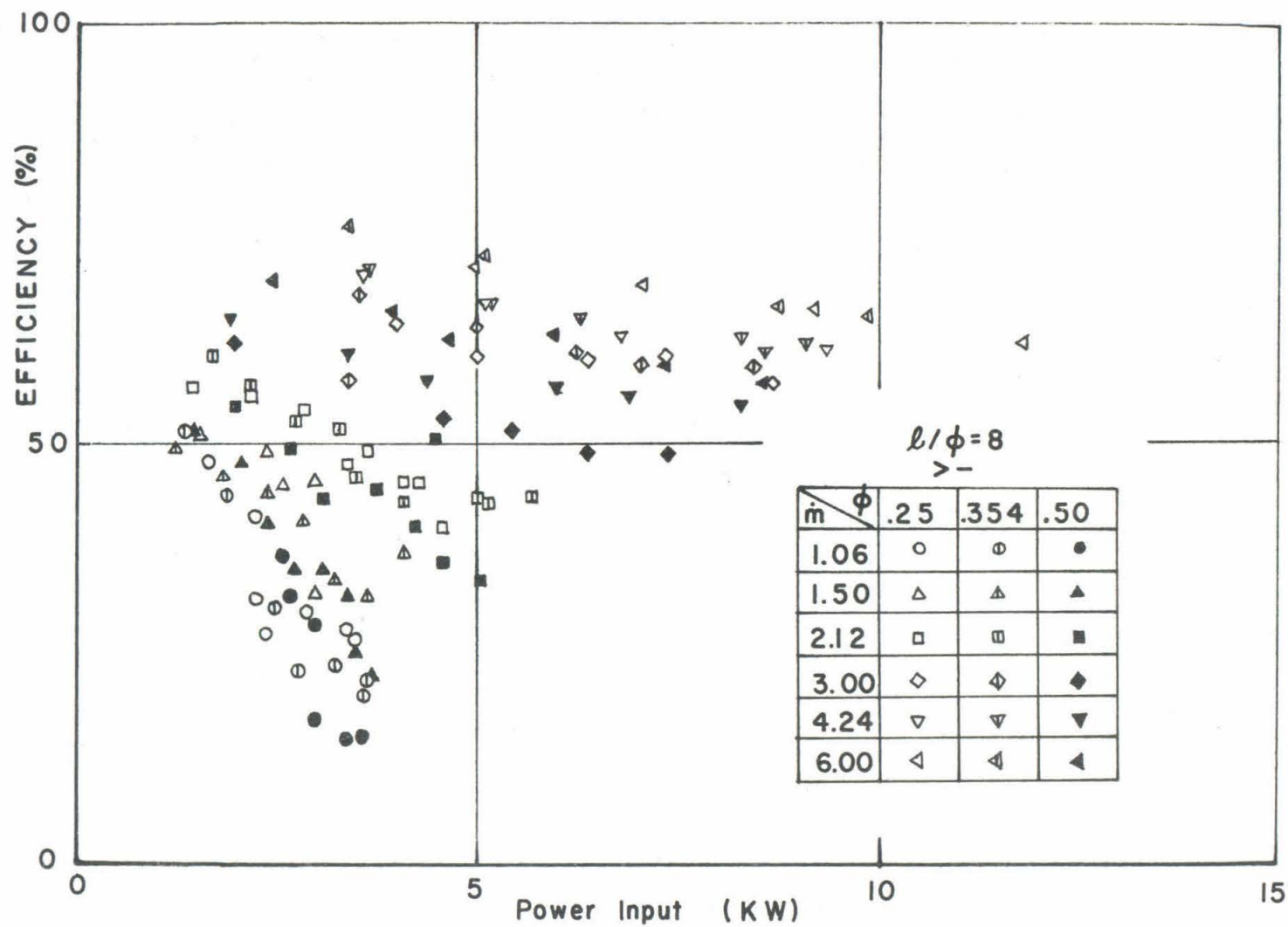


FIG. 16 EFFICIENCY  $\eta$  VS. GROSS POWER INPUT

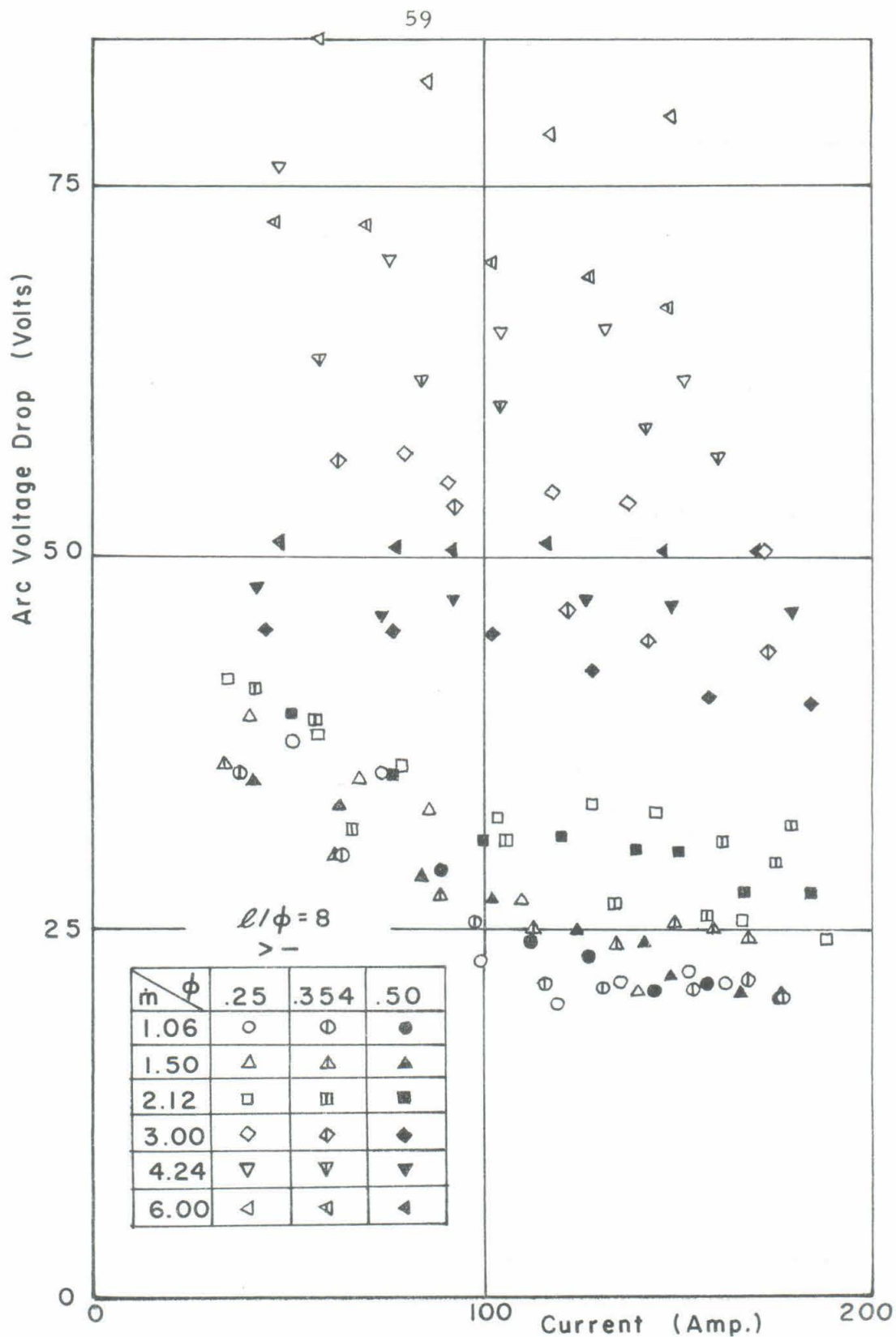
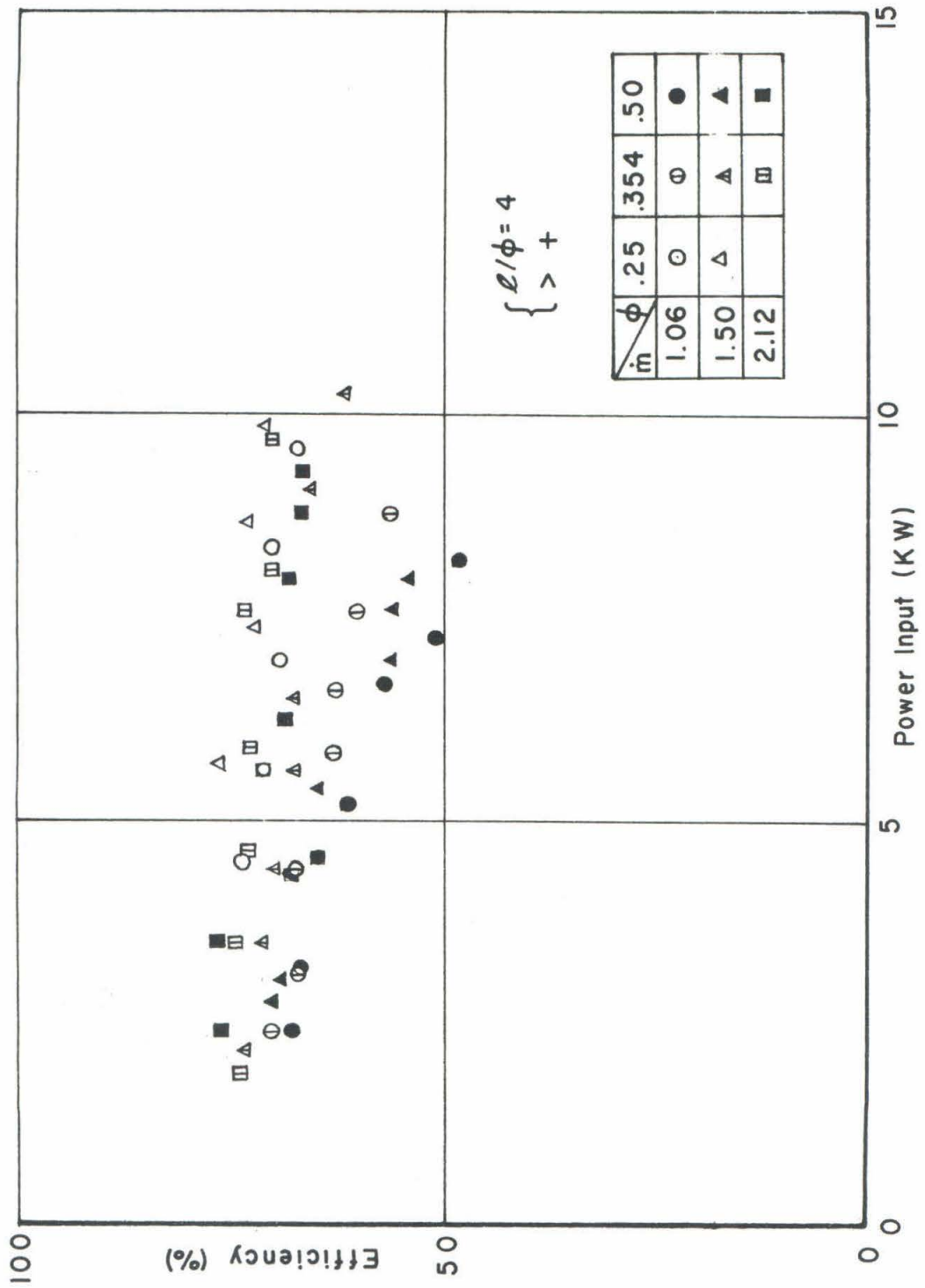


FIG. 17 ARC VOLTAGE DROP VS. CURRENT

FIG. 18 EFFICIENCY  $\eta$  VS. GROSS POWER INPUT

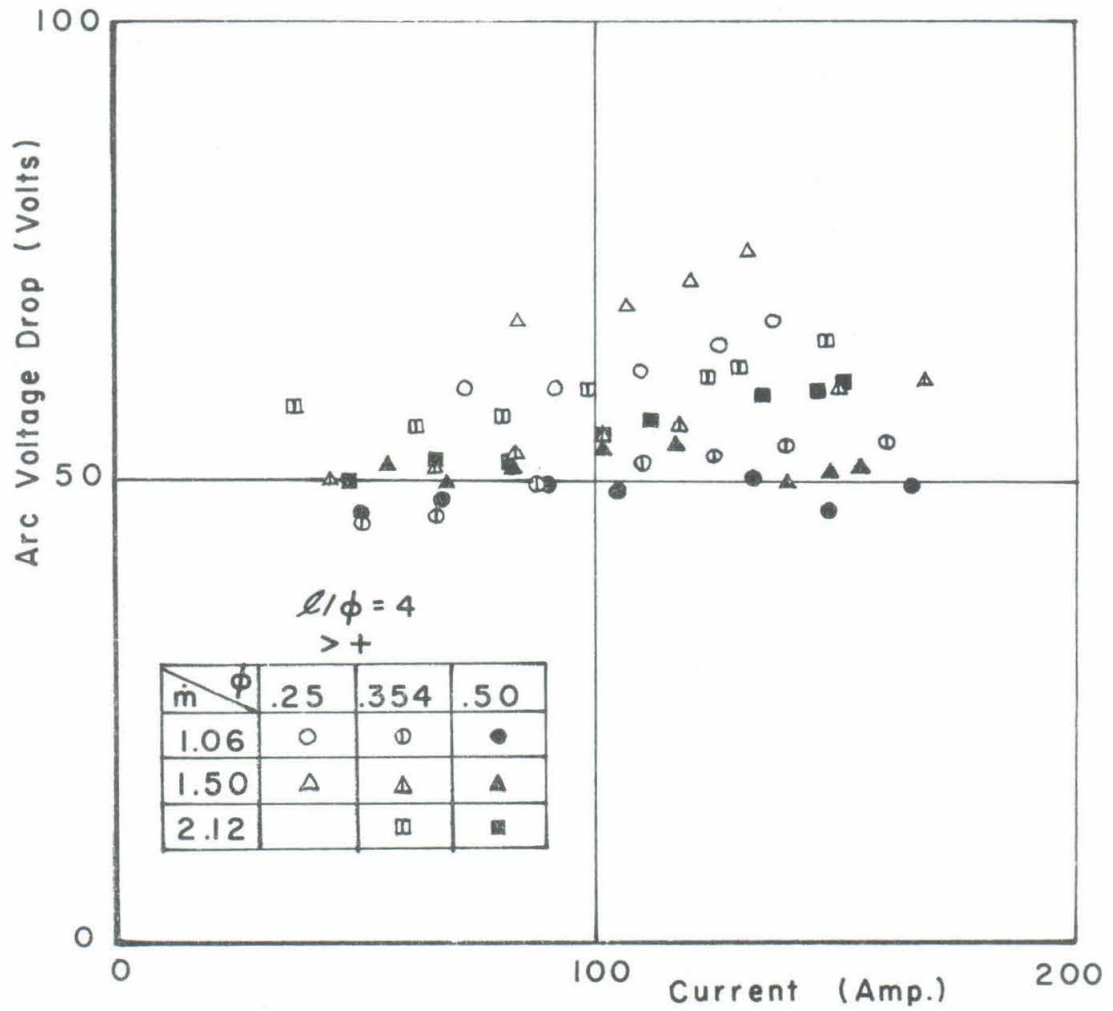


FIG. 19 ARC VOLTAGE DROP VS. CURRENT



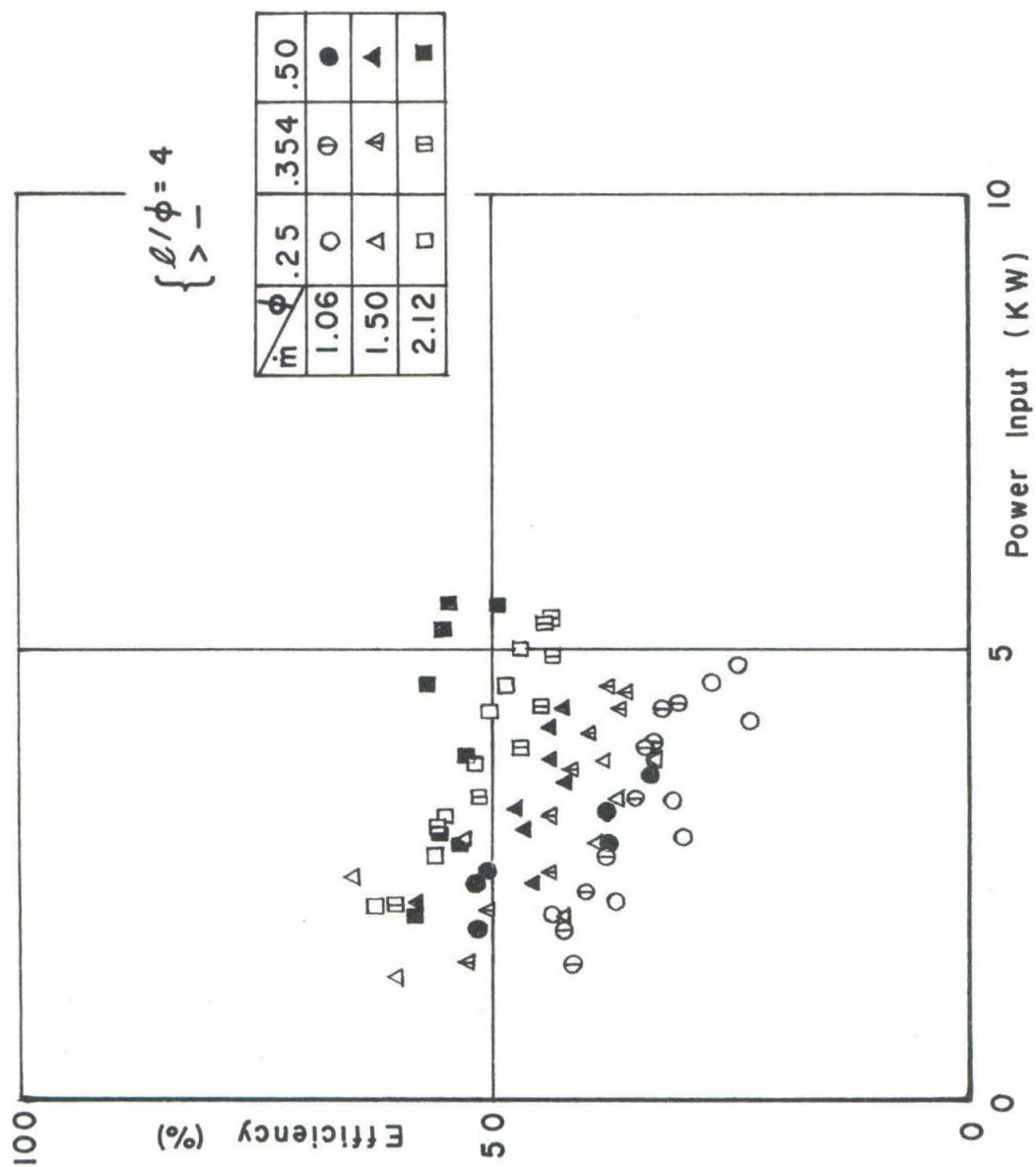


FIG. 20 EFFICIENCY VS. GROSS POWER INPUT

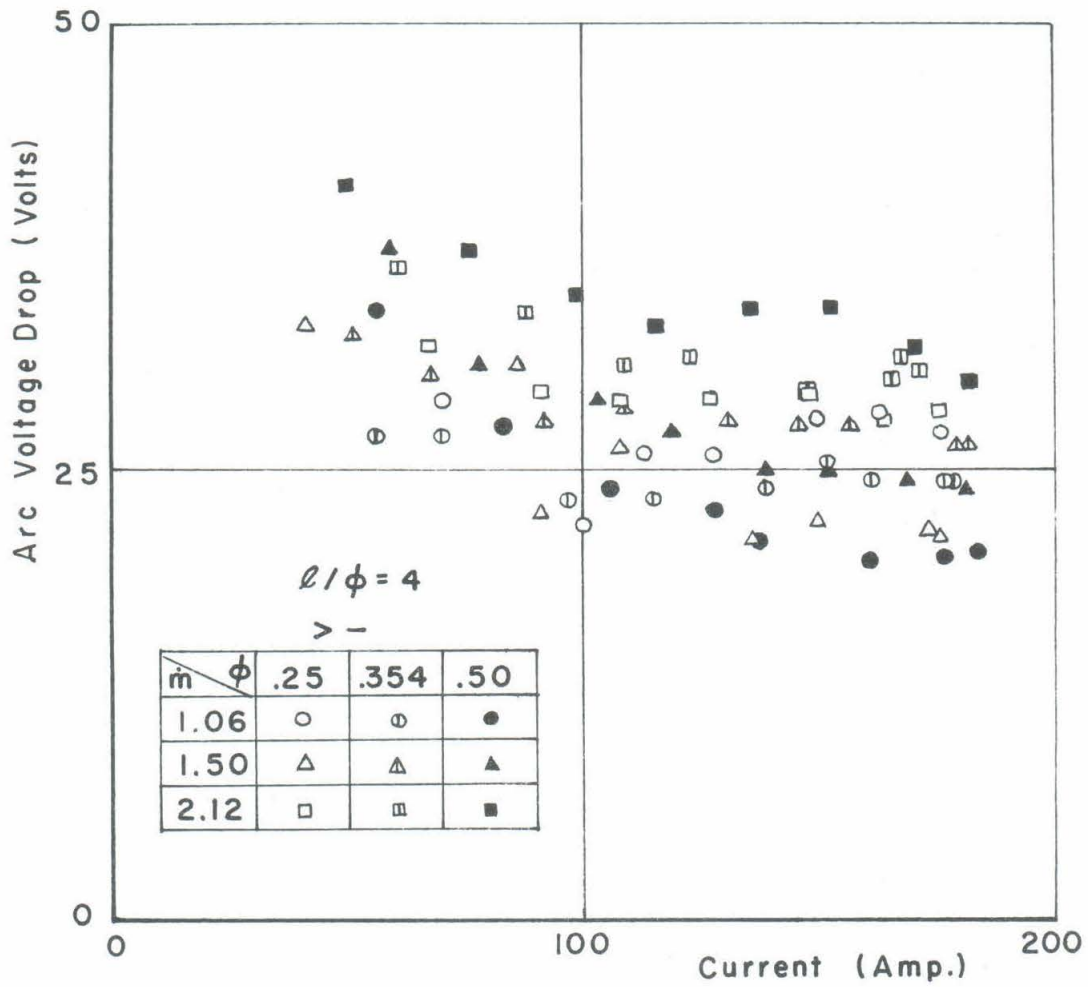


FIG. 21 ARC VOLTAGE DROP VS. CURRENT

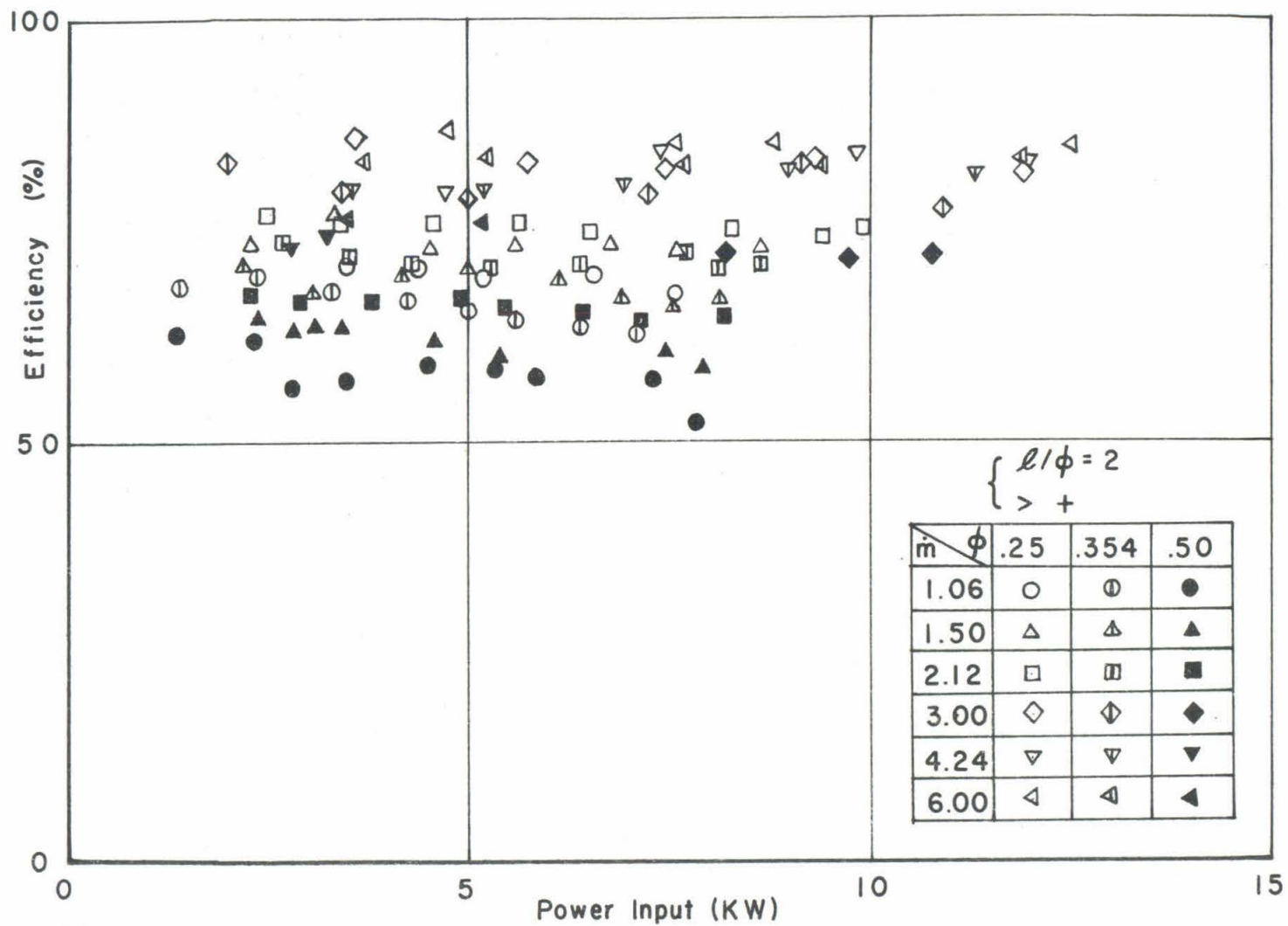


FIG. 22 EFFICIENCY  $\eta$  VS. GROSS POWER INPUT

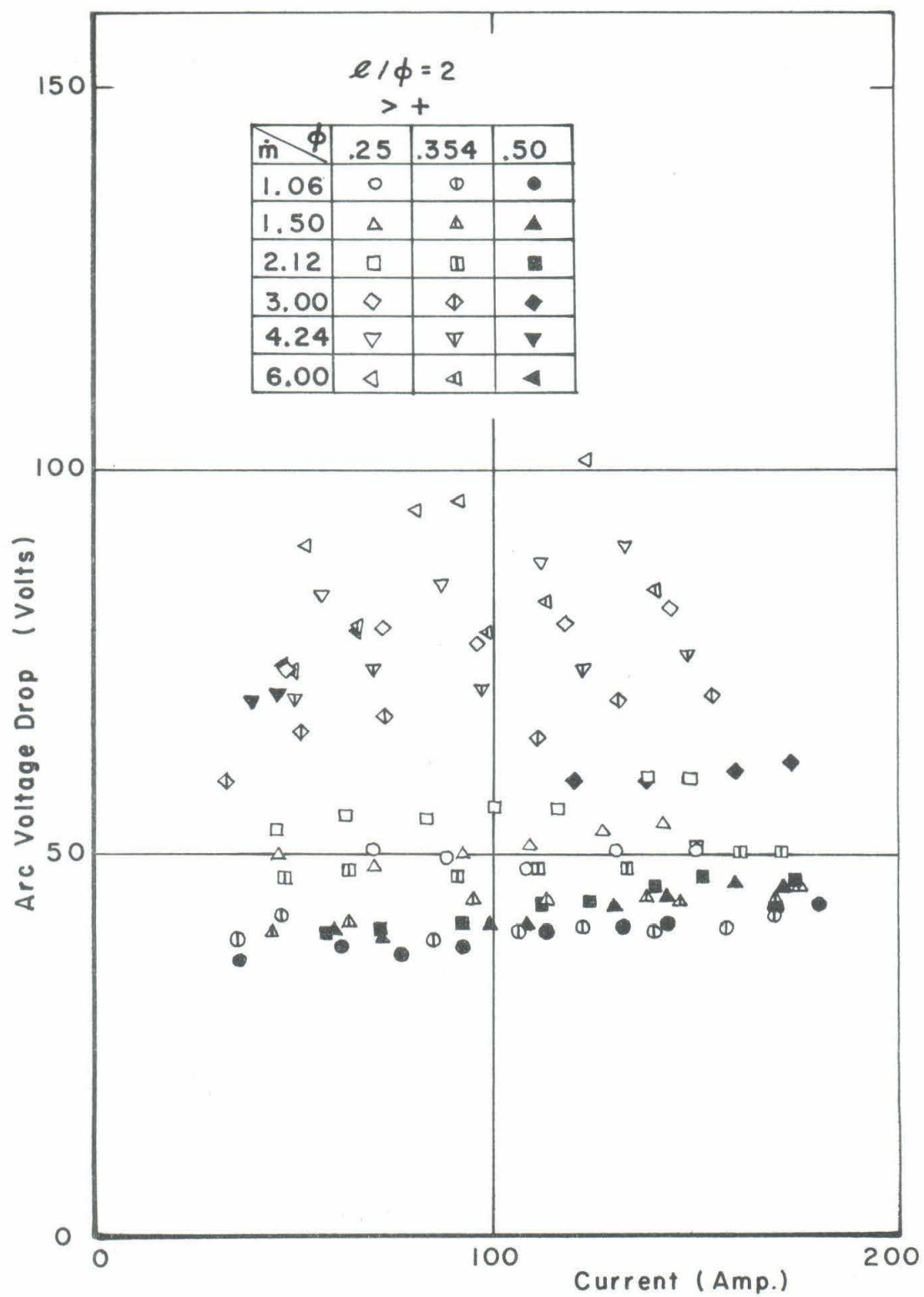


FIG. 23 ARC VOLTAGE DROP VS. CURRENT

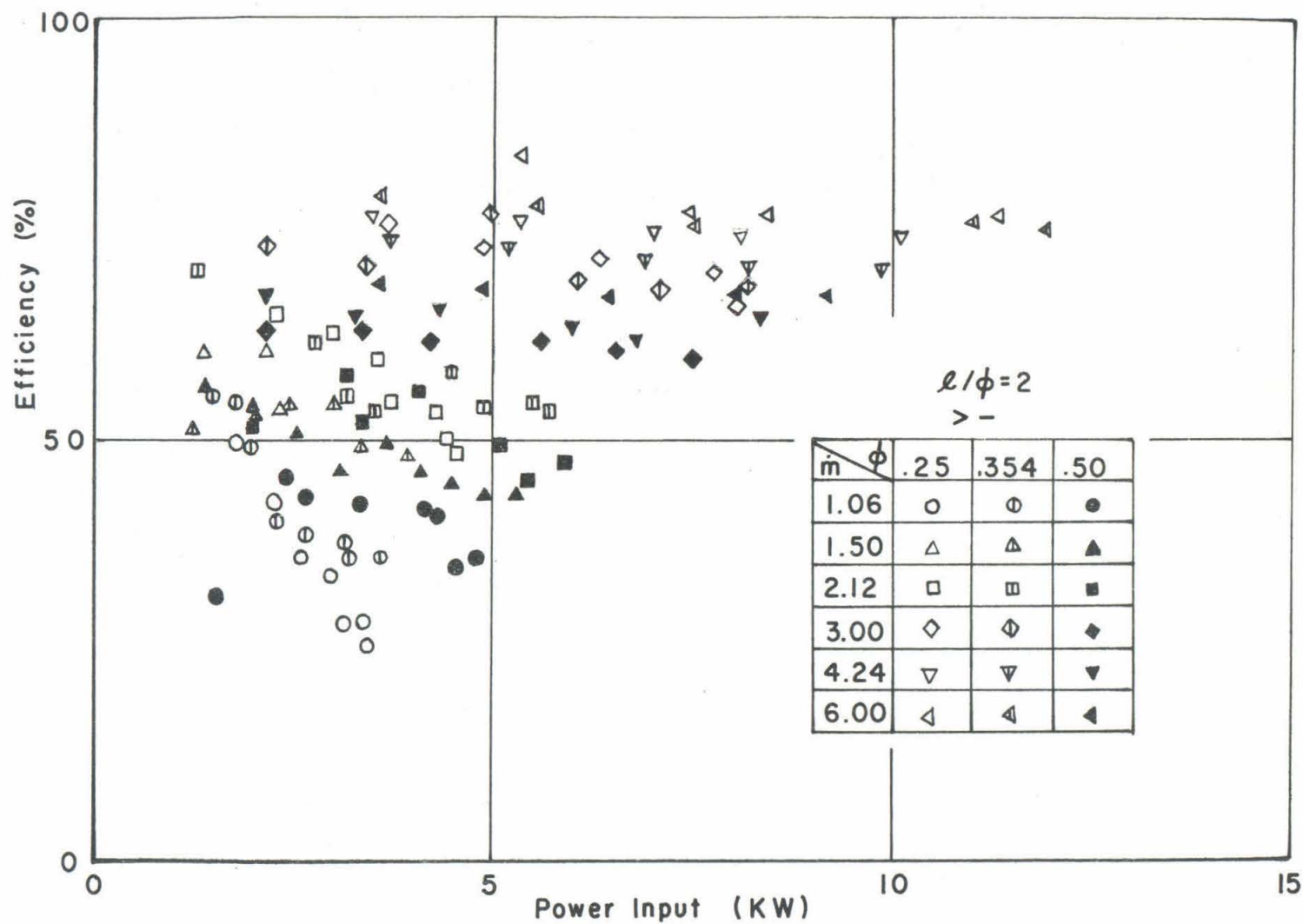


FIG.24 EFFICIENCY  $\eta$  VS. GROSS POWER INPUT



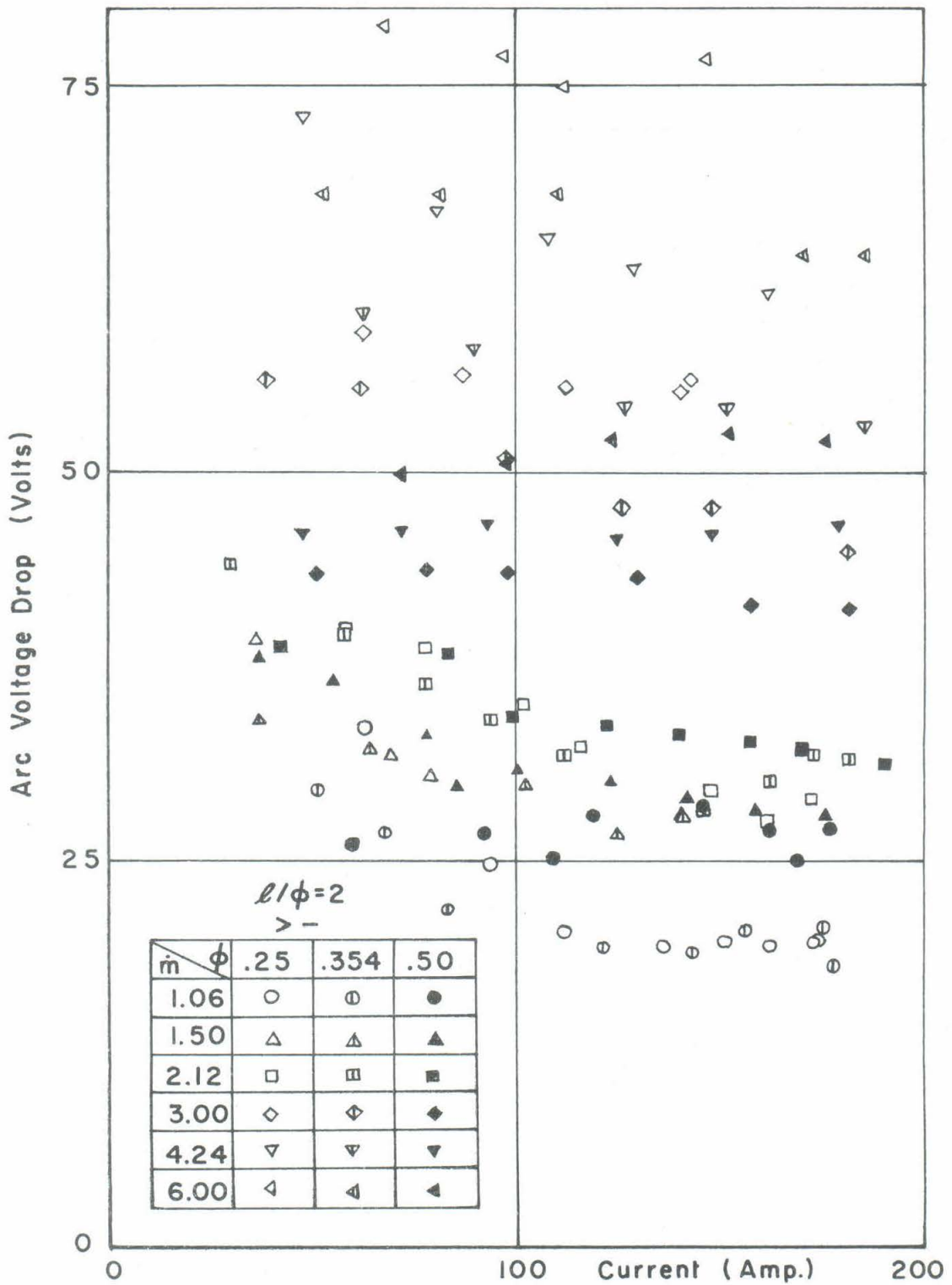


FIG. 25 ARC VOLTAGE DROP VS. CURRENT

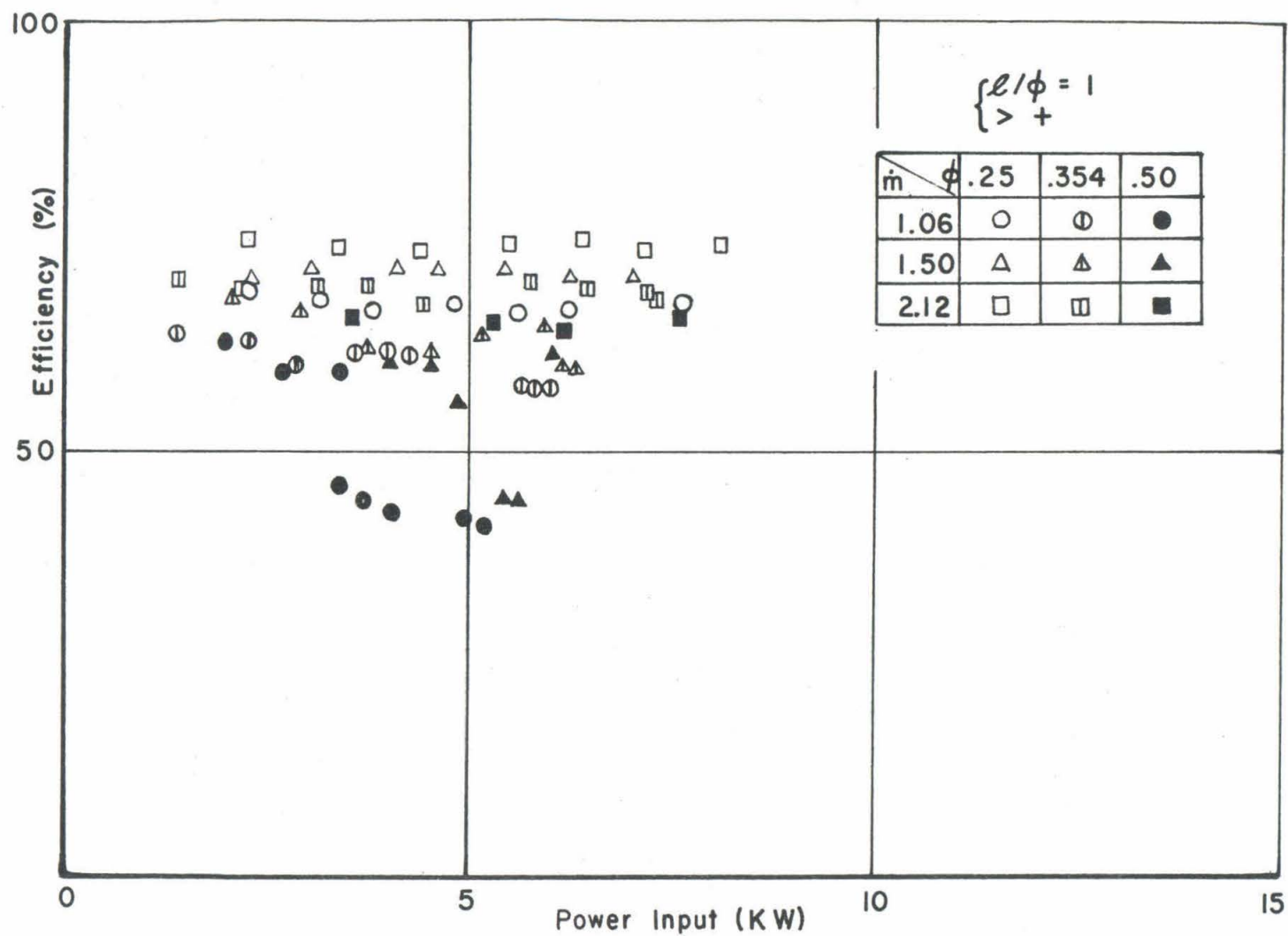


FIG. 26 EFFICIENCY  $\eta$  VS. GROSS POWER INPUT

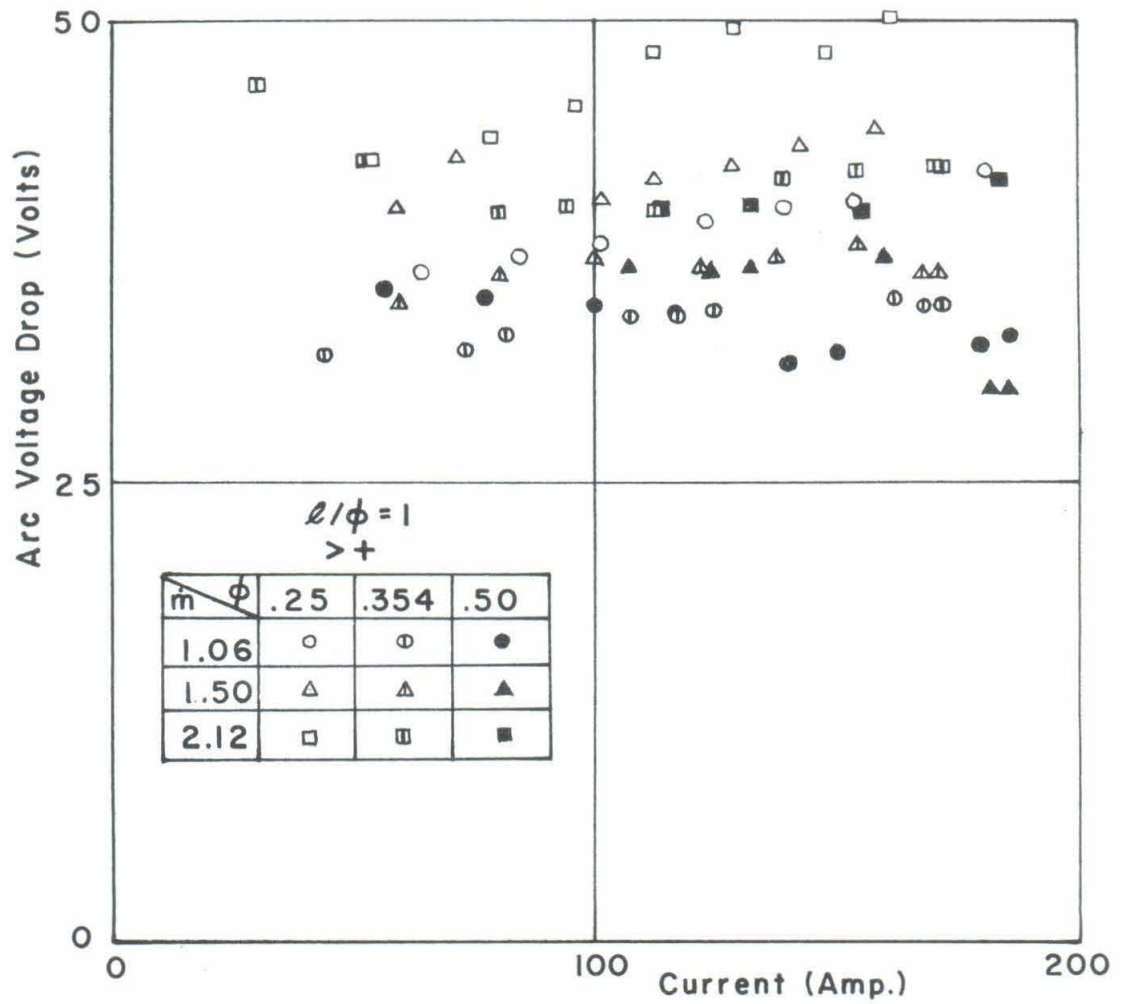


FIG. 27 ARC VOLTAGE DROP VS. CURRENT

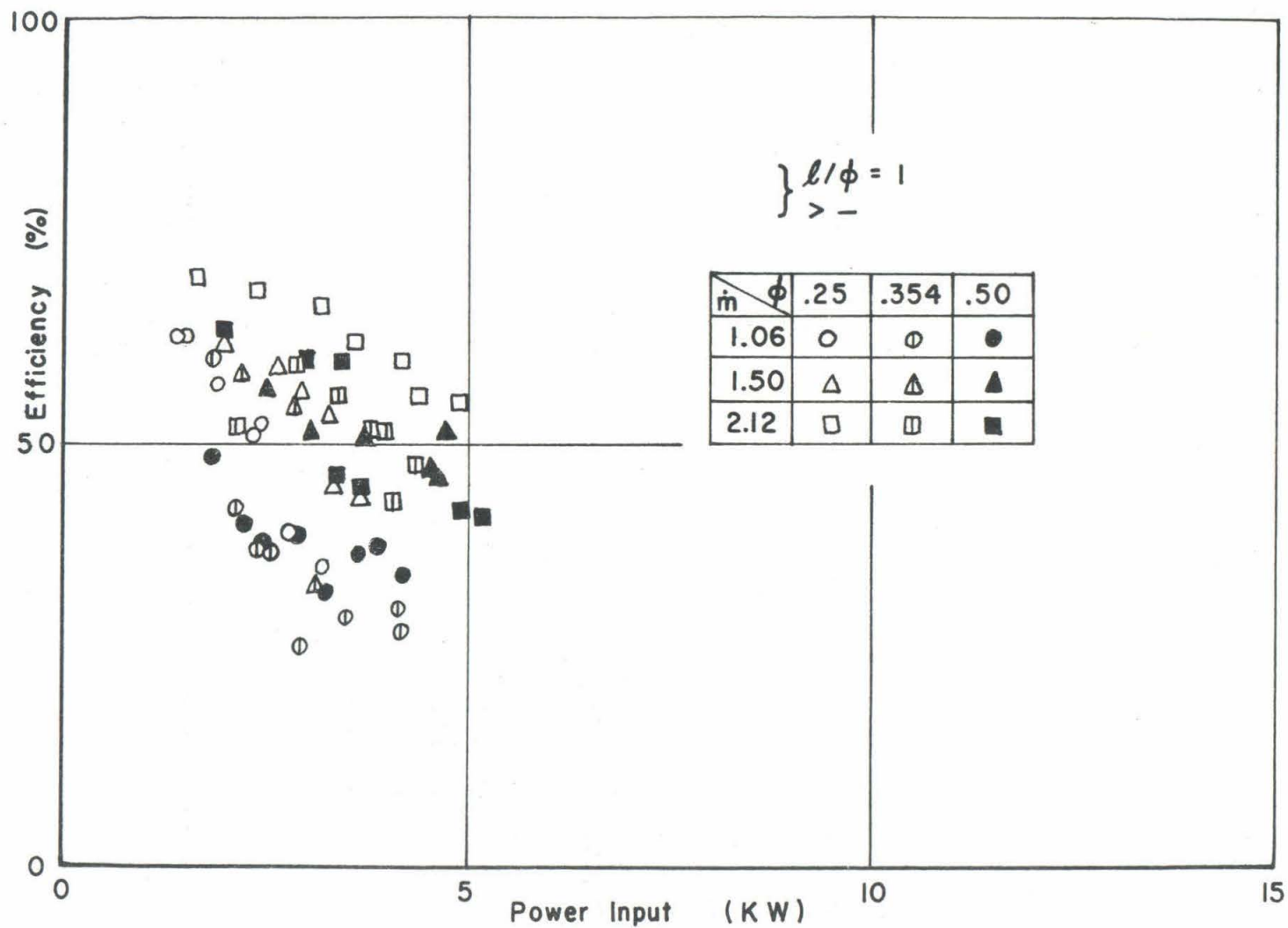


FIG.28 EFFICIENCY  $\eta$  VS. GROSS POWER INPUT

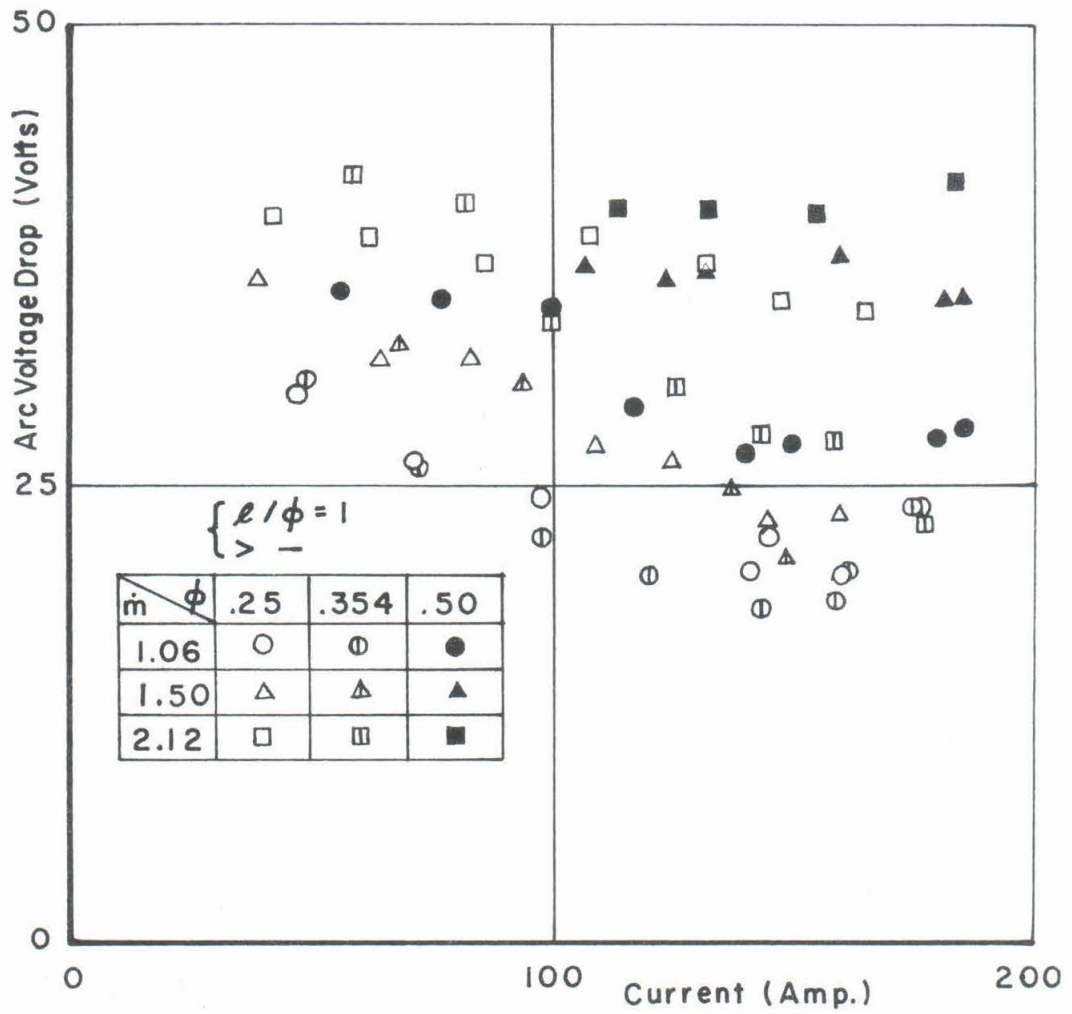


FIG.29 ARC VOLTAGE DROP VS. CURRENT



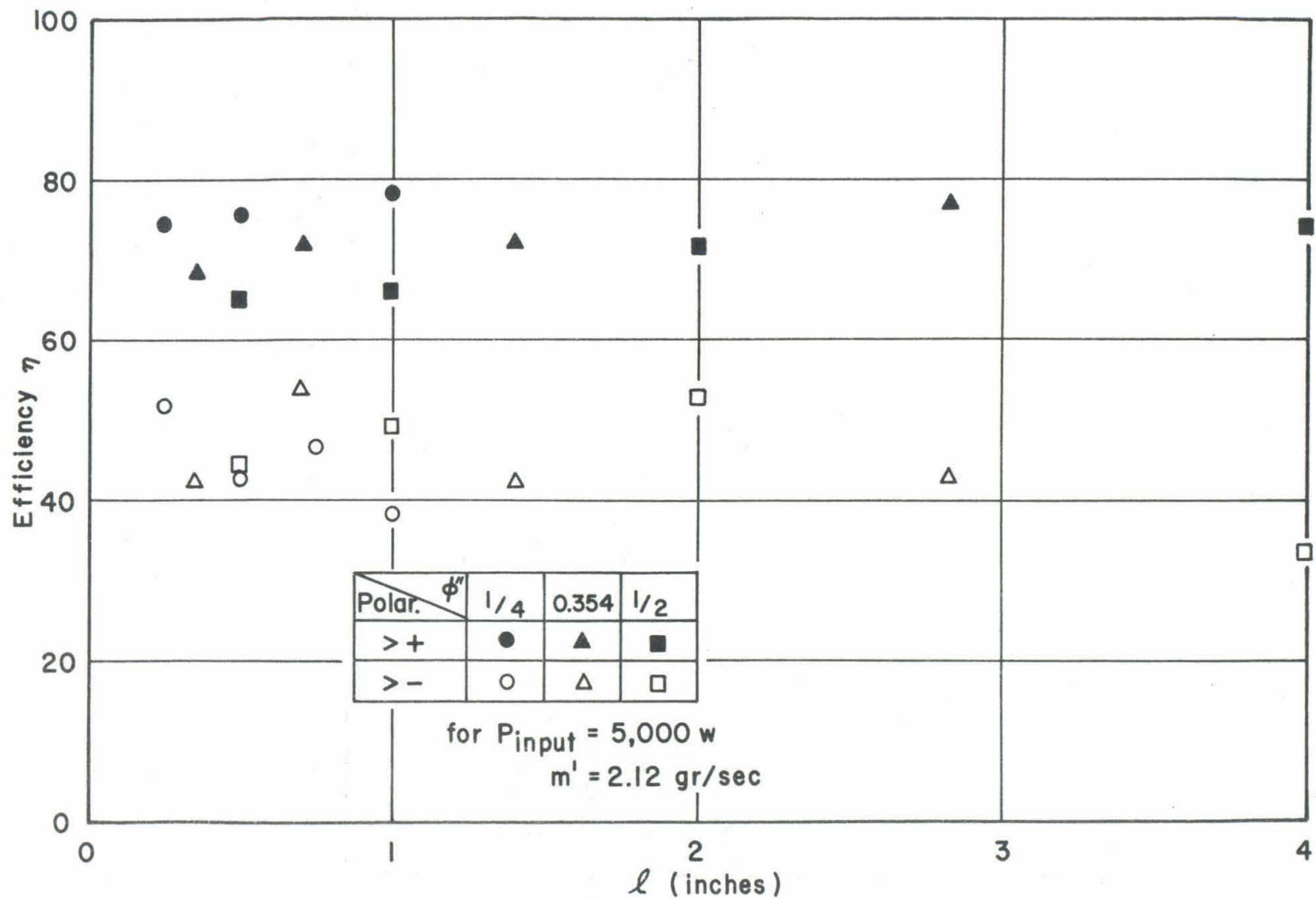
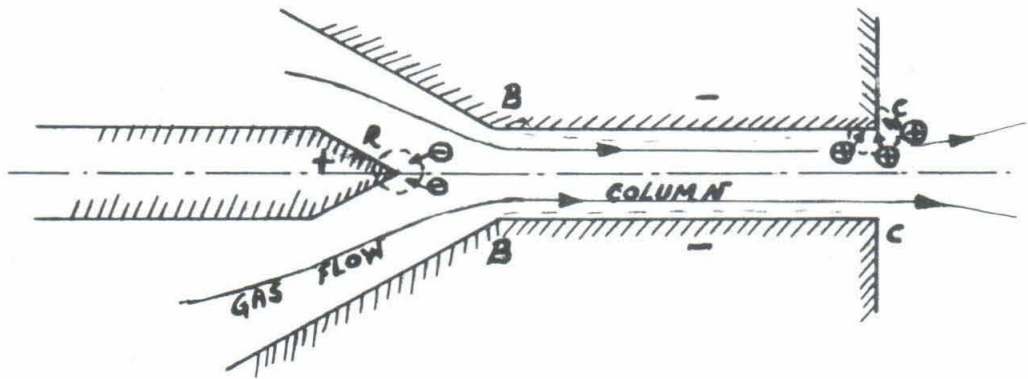
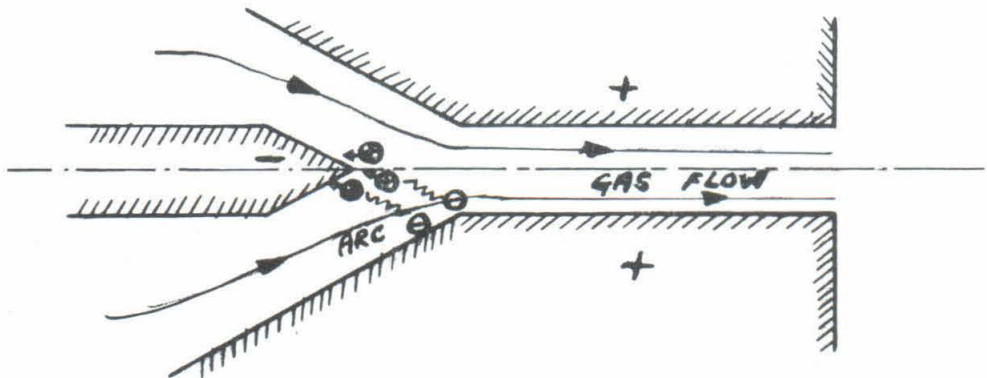


FIG. 30 EFFICIENCY VS. LENGTH  $\ell$  OF CONSTRICTING CHANNEL



>+ Configuration.



>- Configuration.

Fig. 31

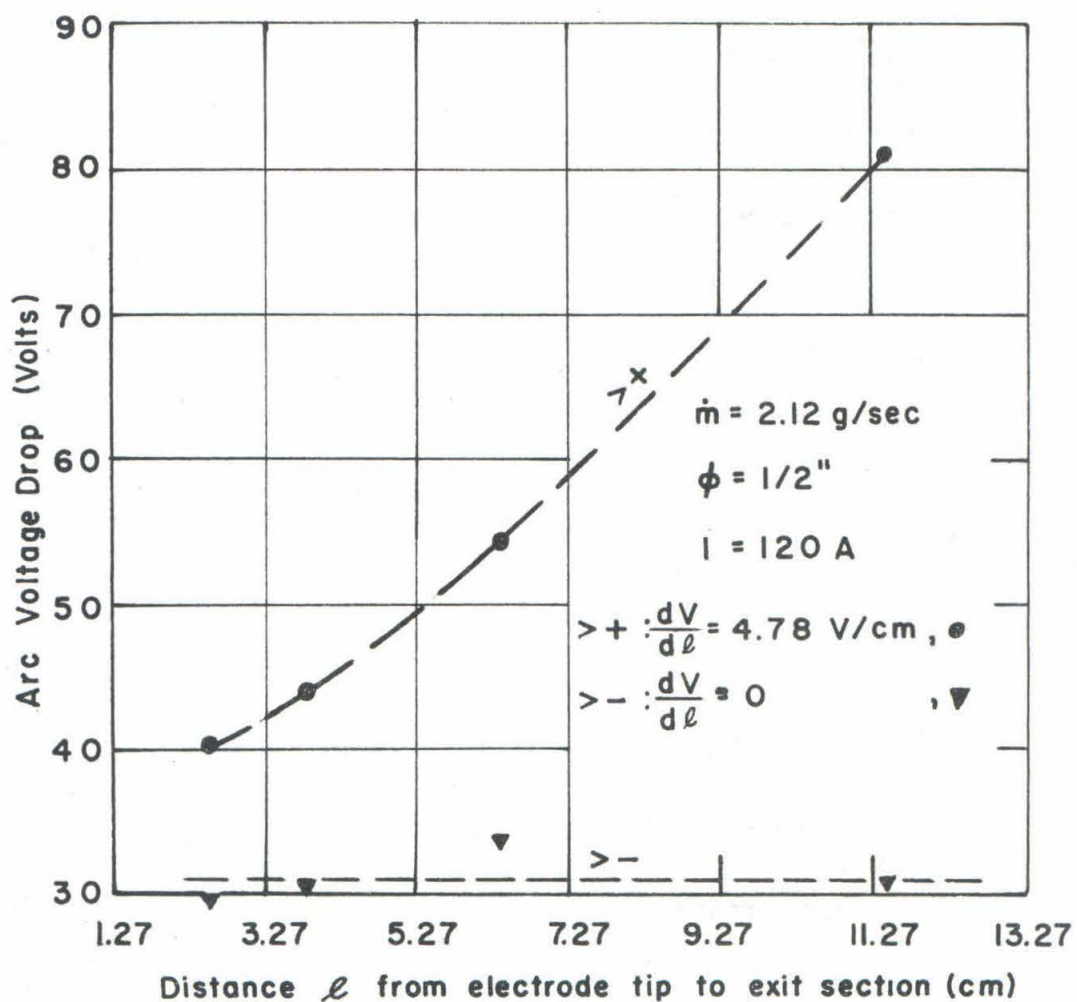


FIG. 32 ARC VOLTAGE DROP VS. DISTANCE TIP-EXIT SECTION

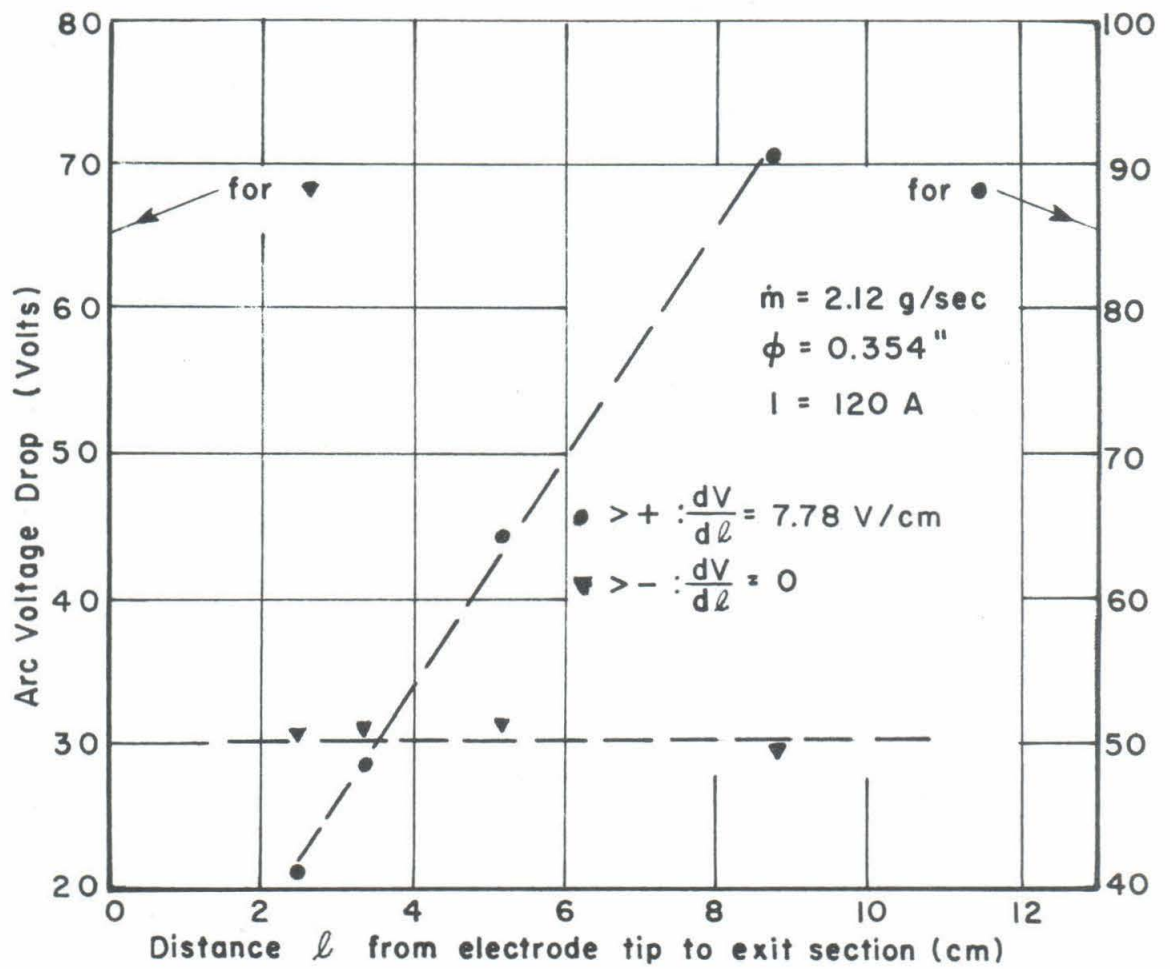


FIG. 33 ARC VOLTAGE DROP VS. DISTANCE TIP-EXIT SECTION

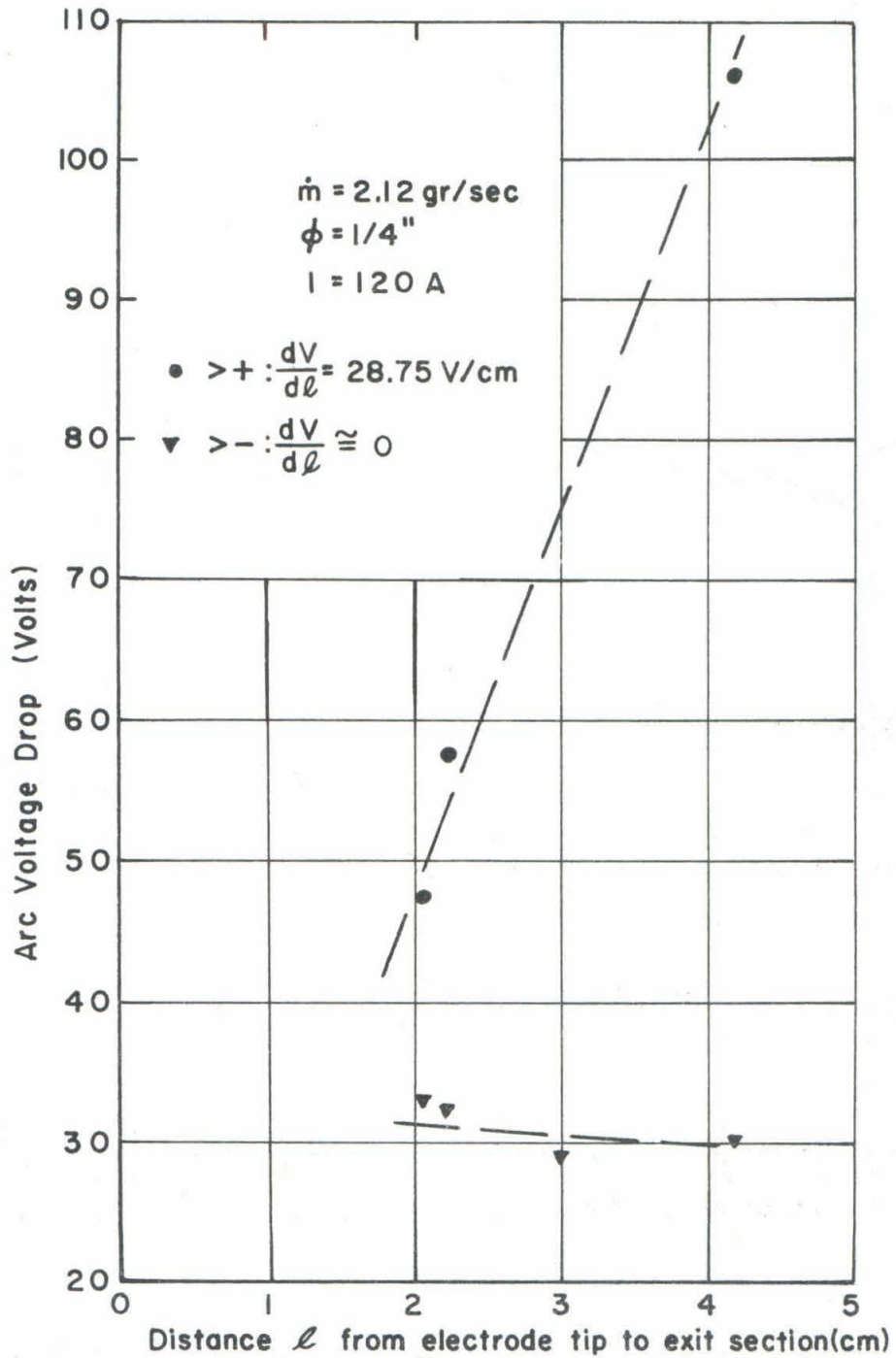


FIG. 34 ARC VOLTAGE DROP VS. DISTANCE TIP-EXIT SECTION



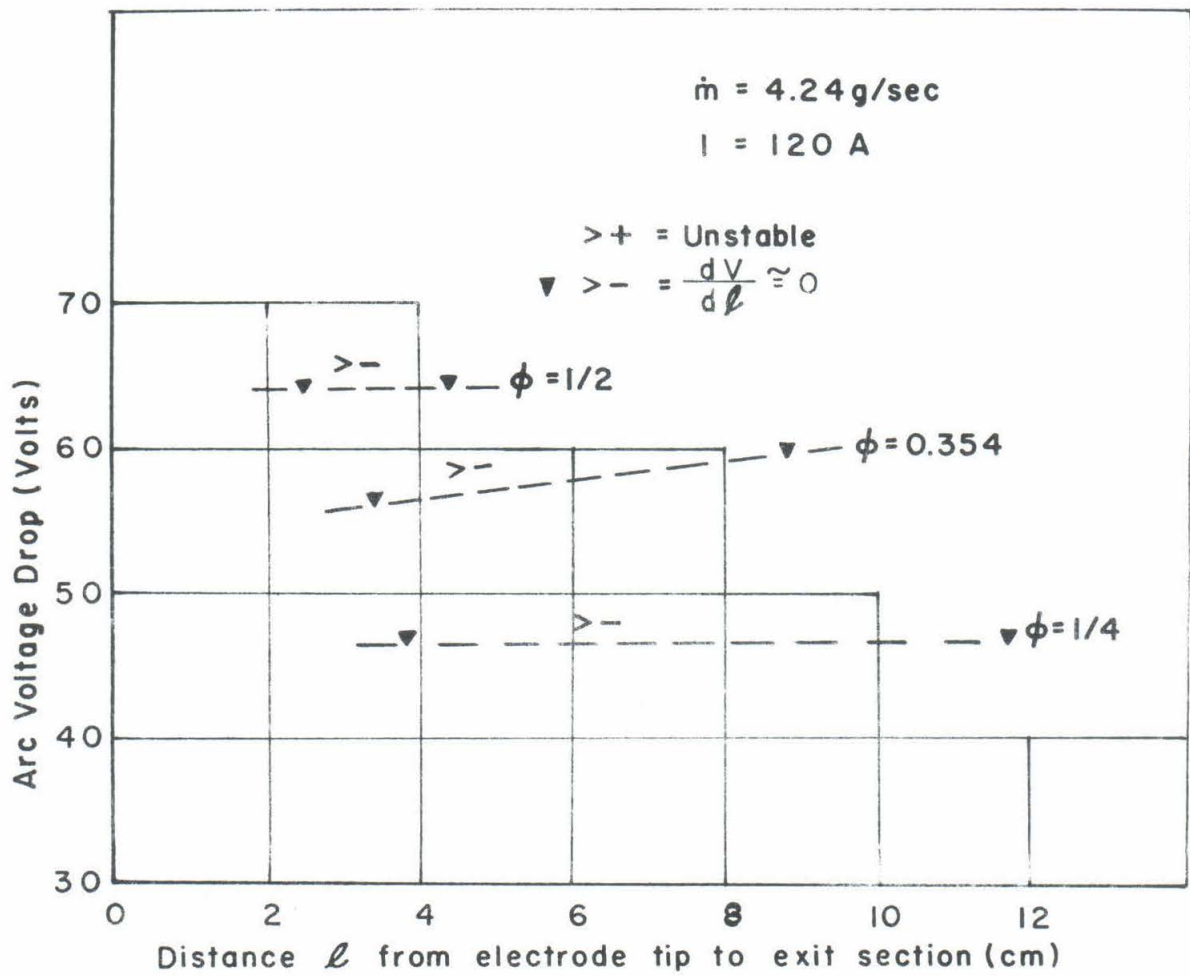


FIG. 35 ARC VOLTAGE DROP VS. DISTANCE TIP-EXIT SECTION



## DISTRIBUTION LIST

### United States Army

U. S. Army Research Office (Durham)  
Box CM, Duke Station  
Durham, North Carolina  
Attention: Information Processing Office  
20 copies

Army Rocket and Guided Missile Agency  
U. S. Army Ordnance Missile Command  
Redstone Arsenal  
Alabama  
Attention: Technical Library  
Attention: Mr. John Morrow  
ORDXR-RMO

Commander  
Army Ballistic Missile Agency  
Redstone Arsenal  
Alabama  
Attention: ORDAB-IPL

Los Angeles Ordnance District  
55 South Grand Avenue  
Pasadena 2, California  
Attention: Mr. John D. Flanagan,  
Chief of Basic Research Section  
Research Branch  
2 copies

Chief of Ordnance  
Department of the Army  
ORDTB - Ballistic Section  
The Pentagon  
Washington 25, D. C.  
Attention: Mr. George Stetson

Office of the Chief of Research and  
Development  
Department of the Army  
Army Research Office  
Washington 25, D. C.  
Attention: Chief, Research Support Division

Commanding Officer  
Diamond Ordnance Fuze Laboratories  
Washington 25, D. C.  
Attention: ORDTL 012

U. S. Army Ordnance  
Ballistic Research Laboratories  
Aberdeen Proving Ground  
Maryland  
Attention: Dr. Joseph Sternberg, Chief  
Exterior Ballistics Laboratory  
Attention: Dr. Raymond Sedney  
Exterior Ballistics Laboratory

Commanding General  
White Sands Missile Range  
New Mexico  
Attention: Technical Library

United States Air Force  
Air Research and Development Command

Aeronautical Research Laboratories  
Air Force Research Division  
Air Research and Development Command  
United States Air Force  
Wright-Patterson Air Force Base  
Ohio  
Attention: Mr. Fred L. Daum, RRLD  
Attention: Dr. Karl Gottfried Guderley, RRLM  
Attention: Dr. Roscoe H. Mills, RRLD  
Attention: RRL

Wright Air Development Division  
Air Research and Development Command  
United States Air Force  
Wright-Patterson Air Force Base  
Ohio  
Attention: WADD (WWAD - Library)  
Attention: WADD (WWFEA - Reports Unit)  
Attention: ASD (ASRMDF - Mr. Philip P. Antonatos)

Air Force Office of Scientific Research  
Air Research and Development Command  
United States Air Force  
Washington 25, D. C.  
Attention: Mechanics Division; Milton Rogers, Chief  
Attention: SRGL (2 copies)

Directorate of Research Analysis  
Air Force Office of Scientific Research  
Air Research and Development Command  
United States Air Force  
Holloman Air Force Base  
New Mexico  
Attention: SRLS, Dr. Gerhard R. Eber

Air Force Ballistic Missile Division  
Air Research and Development Command  
United States Air Force  
Air Force Unit Post Office  
Los Angeles 45, California  
Attention: Advanced Systems Division (WDTV-3); Major E. W. Geniesse, Jr.  
Attention: Penetration Division (WDTV-4); 1/Lt. H. E. Hunter  
Attention: AVCO Re-entry Vehicles Division (WDTV-1); Capt. G. S. Lewis, Jr.

Air Research and Development Command  
United States Air Force  
Eglin Air Force Base  
Florida  
Attention: APGC (PGTRI, Technical Library)

Armed Services Technical Information Agency  
Air Research and Development Command  
United States Air Force  
Arlington Hall Station  
Arlington 12, Virginia  
Attention: ASTIA (TIPCA)  
10 copies

## United States Navy

Director  
U. S. Naval Research Laboratory  
Washington 25, D. C.

U. S. Naval Ordnance Laboratory  
White Oak  
Silver Spring, Maryland  
Attention: Dr. R. Kenneth Lobb  
Aeroballistics Program Chief

Attention: Dr. A. E. Seigel  
Chief, Ballistics Department

Attention: Dr. R. E. Wilson  
Associate Technical Director  
(Aeroballistics)

U. S. Naval Weapons Laboratory  
Dahlgren, Virginia  
Attention: Technical Library

U. S. Navy Department  
David Taylor Model Basin  
Applied Mathematics Laboratory  
Washington 7, D. C.  
Attention: Dr. F. N. Frenkiel

## National Aeronautics and Space Administration

NASA  
Headquarters  
1520 H Street, Northwest  
Washington 25, D. C.  
Attention: Dr. H. H. Kurzweg  
Assistant Director of Research

NASA  
George C. Marshall Space Flight Center  
Huntsville, Alabama  
Attention: Dr. Ernst D. Geissler, Director, Aeroballistics Division  
Attention: M-AERO-A, Mr. Werner K. Dahm  
Attention: Aeroballistics Division, M-AERO-E, Mr. T. G. Reed (3 copies)

NASA  
Langley Research Center  
Langley Field, Virginia  
Attention: Librarian

Attention: Mr. Clinton E. Brown, Chief, Theoretical Mechanics Division, Bldg. 1212

Attention: Dr. Adolf Busemann

Attention: Mr. Charles H. McLellan, 11-Inch Hypersonic Tunnel Section

NASA  
Ames Research Center  
Moffett Field, California  
Attention: Library

NASA  
Lewis Research Center  
21000 Brookpark Road  
Cleveland 35, Ohio  
Attention: Library, Mr. George Mandel (2 copies)

## Miscellaneous Government Agencies

United States Atomic Energy Commission  
P. O. Box 62  
Oak Ridge, Tennessee  
Attention: Library

U. S. Department of Commerce  
National Bureau of Standards  
Washington 25, D. C.  
Attention: Dr. G. B. Schubauer  
Chief, Fluid Mechanics Sec.



## Universities and Non-Profit Organizations

Brown University  
Division of Applied Mathematics  
Providence 12, Rhode Island  
Attention: Professor R. E. Meyer

Brown University  
Division of Engineering  
Providence 12, Rhode Island  
Attention: Dr. Ronald F. Probst

University of California at Berkeley  
Aeronautical Sciences Department  
Room 203, Mechanics Building  
Berkeley 4, California  
Attention: Professor S. A. Schaaf

University of California  
405 Hilgard Avenue  
Los Angeles 24, California  
Attention: Engineering and Mathematical  
Sciences Library  
Engineering II 8270

University of California  
Department of Engineering  
Los Angeles 24, California  
Attention: Professor A. F. Charwat  
Attention: Dr. N. Rott

Case Institute of Technology  
Department of Mechanical Engineering  
University Circle  
Cleveland 6, Ohio  
Attention: Dr. G. Kuerti

Columbia University  
Department of Mechanical Engineering  
New York 27, N. Y.  
Attention: Professor Robert A. Gross

Cornell University  
Graduate School of Aeronautical Eng.  
Ithaca, New York  
Attention: Library  
Attention: Dr. William R. Sears

University of Florida  
Department of Aeronautical Engineering  
Gainesville, Florida  
Attention: Professor David T. Williams

Harvard University  
Division of Eng. and App. Physics  
Cambridge 38, Massachusetts  
Attention: Dr. Howard W. Emmons

University of Illinois  
Department of Aeronautical Engineering  
Urbana, Illinois  
Attention: Professor Harold O. Barthel  
Attention: Dr. Allen I. Ormsbee

The Johns Hopkins University  
Applied Physics Laboratory  
8621 Georgia Avenue  
Silver Spring, Maryland  
Attention: Dr. L. L. Cronvich  
Attention: Dr. F. K. Hill

The Johns Hopkins University  
Department of Mechanics  
Baltimore 18, Maryland  
Attention: Dr. Francis H. Clauser  
Attention: Dr. Stanley Corrsin  
Attention: Professor L. S. G. Kovasznay

Lehigh University  
Department of Physics  
Bethlehem, Pennsylvania  
Attention: Dr. Raymond J. Emrich

University of Maryland  
Department of Aeronautical Engineering  
College Park, Maryland  
Attention: Professor S. F. Shen

University of Maryland  
Institute for Fluid Dynamics and  
Applied Mathematics  
College Park, Maryland  
Attention: Director  
Attention: Professor J. M. Burgers  
Attention: Professor Francis R. Hama  
Attention: Professor S. I. Pai

Massachusetts Institute of Technology  
Department of Aeronautics and  
Astronautics  
Cambridge 39, Massachusetts  
Attention: Prof. E. Mollo-Christensen  
Room 33-412  
Attention: Dr. Leon Trilling  
Room 33-412

Massachusetts Institute of Technology  
Department of Aeronautics and  
Astronautics  
Aerophysics Laboratory  
560 Memorial Drive  
Cambridge 39, Massachusetts  
Attention: Dr. Morton Finston

Massachusetts Institute of Technology  
Department of Mathematics  
Cambridge 39, Massachusetts  
Attention: Professor C. C. Lin  
Attention: Dr. George B. Whitham

Massachusetts Institute of Technology  
Department of Mechanical Engineering  
Cambridge 39, Massachusetts  
Attention: Dr. A. H. Shapiro  
Attention: Dr. H. Guyford Stever  
Room 3-174

University of Michigan  
Ann Arbor, Michigan  
Attention: Engineering Library

University of Michigan  
Willow Run Laboratories  
P. O. Box 618  
Ann Arbor, Michigan  
Attention: BAMIRAC Library  
Mr. Richard Jamron, Head  
Information Handling Group

University of Michigan  
Aeronautical Engineering Laboratories  
Aerodynamics Laboratory  
North Campus  
Ann Arbor, Michigan  
Attention: Mr. James L. Amick

University of Michigan  
Aeronautical Engineering Laboratories  
Aircraft Propulsion Laboratory  
North Campus  
Ann Arbor, Michigan  
Attention: Professor J. A. Nicholls

University of Michigan  
Department of Aeronautical and  
Astronautical Engineering  
Ann Arbor, Michigan  
Attention: Dr. Arnold M. Kuethe  
Attention: Professor V. C. Liu  
Attention: Professor William W. Willmarth

University of Michigan  
Department of Physics  
Ann Arbor, Michigan  
Attention: Dr. O. Laporte

University of Minnesota  
Institute of Technology  
Rosemount Aeronautical Laboratories  
Rosemount, Minnesota  
Attention: Mrs. Linda Caldon,  
Librarian

New York University  
Institute of Mathematics and Mechanics  
53 Washington Square, South  
New York 12, N. Y.  
Attention: Library

North Carolina State College  
Department of Mechanical Engineering  
Raleigh, North Carolina  
Attention: Professor R. M. Pinkerton

Northwestern University  
The Technological Institute  
Evanston, Illinois  
Attention: Professor Ali Bulent Cambel

The Ohio State University  
Department of Aeronautical and  
Astronautical Engineering  
2036 Neil Avenue  
Columbus 10, Ohio  
Attention: Professor John D. Lee  
Attention: Professor Gavin L. VonEschen

Polytechnic Institute of Brooklyn  
Aerodynamics Laboratory  
527 Atlantic Avenue  
Freeport, New York  
Attention: Library  
Attention: Professor Martin H. Bloom  
Attention: Professor Antonio Ferri  
Attention: Professor Paul A. Libby

Princeton University  
School of Engineering  
James Forrestal Research Center  
Princeton, New Jersey  
Attention: Library  
Attention: Gas Dynamics Laboratory  
Attention: Dr. Seymour Bogdonoff  
Attention: Professor Sin-I Cheng  
Attention: Dr. Luigi Crocco

Purdue University  
School of Aeronautical and Engineering  
Sciences  
West Lafayette, Indiana  
Attention: Aero. and Engineering  
Sciences Library

Rensselaer Polytechnic Institute  
Department of Aeronautical Engineering  
Troy, New York  
Attention: Library  
Attention: Dr. Ting-Yi Li



University of Rochester  
College of Engineering  
Department of Mechanical Engineering  
River Campus Station  
Rochester 20, New York  
Attention: Professor Martin Lessen

Institute of the Aerospace Sciences  
2 East 64th Street  
New York 21, New York  
Attention: Library

University of Southern California  
Engineering Center  
University Park  
Los Angeles 7, California  
Attention: Director  
Attention: Dr. H. T. Yang

University of Southern California  
Engineering Center  
Aeronautical Laboratories Department  
P. O. Box 1001  
Oxnard, California  
Attention: Mr. J. H. Carrington,  
USCEC-ATL

Stanford University  
Department of Aeronautical Engineering  
Stanford, California  
Attention: Professor Daniel Bershader  
Attention: Dr. Milton Van Dyke  
Attention: Prof. Walter G. Vincenti

University of Texas  
Defense Research Laboratory  
P. O. Box 8029  
Austin 12, Texas  
Attention: Dr. M. J. Thompson

University of Virginia  
Department of Physics  
Charlottesville, Virginia  
Attention: Dr. Jesse W. Beams

University of Washington  
Department of Aeronautical Engineering  
Seattle 5, Washington  
Attention: Engineering Librarian  
Attention: Professor R. E. Street

University of Wisconsin  
Theoretical Chemistry Laboratory  
P. O. Box 2127  
Madison 5, Wisconsin  
Attention: Dr. Joseph O. Hirschfelder

Yale University  
Department of Mechanical Engineering  
New Haven, Connecticut  
Attention: Dr. Alan Kistler  
Attention: Dr. Peter Wegener

## Industrial Research Companies

Aeronautical Research Associates  
of Princeton, Inc.  
50 Washington Road  
Princeton, New Jersey  
Attention: Dr. Coleman duP. Donaldson

Aeronutronic  
A Division of Ford Motor Company  
Ford Road  
P. O. Box 697  
Newport Beach, California  
Attention: Dr. L. L. Kavanau  
Advanced Programs Staff

Aerospace Corporation, Inc.  
P. O. Box 95085  
Los Angeles 45, California  
Attention: Dr. Chieh-Chien Chang  
Attention: Dr. J. Logan, Director  
2 copies  
Attention: Dr. H. Mirels

ARO, Inc.  
Arnold Air Force Station  
Tennessee  
Attention: AEDC Library  
Attention: Dr. B. H. Goethert  
Director of Engineering  
Attention: TS(Tl)

ARO, Inc.  
von Karman Gas Dynamics Facility  
Arnold Air Force Station  
Tennessee  
Attention: Dr. J. Lukasiewicz, Chief  
Attention: Mr. J. Leith Potter,  
Manager, Research Branch

AVCO-Everett Research Laboratory  
2385 Revere Beach Parkway  
Everett 49, Massachusetts  
Attention: Barbara A. Spence,  
Technical Librarian

AVCO Research and Advanced  
Development Division  
201 Lowell Street  
Wilmington, Massachusetts  
Attention: Mr. A. Kahane  
Assistant Technical Director  
Attention: Dr. Frederick R. Riddell,  
Tech. Ass't. to Pres. -S. Tec.

Boeing Airplane Company  
Aero-Space Division  
Seattle 24, Washington  
Attention: Library 13-84

CONVAIR  
A Division of General Dynamics Corp.  
Astronautics Division  
P. O. Box 1128  
San Diego 12, California  
Attention: Mr. K. J. Bossart, Tech. Dir.  
Attention: Mr. W. B. Mitchell, 595-10

CONVAIR  
A Division of General Dynamics Corp.  
Scientific Research Laboratory  
5001 Kearny Villa Road  
San Diego 11, California  
Attention: Mr. Merwin Sibulkin  
Staff Scientist

CONVAIR  
A Division of General Dynamics Corp.  
Aerospace Technology Section  
P. O. Box 748  
Fort Worth, Texas  
Attention: Mr. R. C. Frost  
Dept. 6-1  
Mail Zone E63

CONVAIR  
A Division of General Dynamics Corp.  
Fort Worth, Texas  
Attention: Mr. A. P. Madsen  
Aerodynamics Group Eng.  
Mail Zone E63  
Attention: Mr. W. G. McMullen  
Attention: Mr. Robert H. Widmer

CONVAIR  
A Division of General Dynamics Corp.  
Daingerfield, Texas  
Attention: Mr. J. E. McMichael  
Chief, Jet Engine Department

Cornell Aeronautical Laboratory  
P. O. Box 235  
Buffalo 21, New York  
Attention: Library  
Attention: Dr. A. H. Flax  
Attention: Mr. A. Hertzberg  
Head, Aerodynamic Research



Douglas Aircraft Company, Inc.  
Missiles and Space Systems  
3000 Ocean Park Blvd.  
Santa Monica, California  
Attention: Library  
Chief,  
Aero/Astrodynamics Section  
2 copies  
Attention: Mr. R. J. Gunkel  
Chief,  
Aero/Astrodynamics Section

Douglas Aircraft Company, Inc.  
827 Lapham Street  
El Segundo, California  
Attention: Dr. A. M. O. Smith

General Dynamics/Astronautics  
Space Sciences Section  
P. O. Box 1128  
San Diego 12, California  
Attention: Dr. Hideo Yoshihara  
Mail Zone 596-7

General Electric Company (MSVD)  
Space Technology Center  
Space Sciences Laboratory  
King of Prussia, Pennsylvania  
Attention: Dr. H. Lew

General Electric Company  
Research Laboratory  
P. O. Box 1088  
Schenectady, New York  
Attention: Dr. Henry T. Nagamatsu

Giannini Controls Corporation  
1600 South Mountain Avenue  
Duarte, California  
Attention: Library

Grumman Aircraft Engineering Corp.  
Bethpage, New York  
Attention: Mr. Charles Tilgner, Jr.

Hughes Aircraft Company  
Culver City, California  
Attention: Mr. E. O. Marriott  
Manager, Aerodynamics Dept.

Lockheed Aircraft Corporation  
Lockheed Missiles and Space Company  
Technical Information Center (50-14)  
3251 Hanover Street  
Palo Alto, California  
Attention: Dr. W. A. Kozumplik  
3 copies

Lockheed Aircraft Corporation  
Lockheed Missiles and Space Company  
P. O. Box 504  
Sunnyvale, California  
Attention: Mr. R. Smelt,  
Chief Scientist

Lockheed Aircraft Corporation  
Lockheed Missile Systems Company  
Palo Alto, California  
Attention: Mr. Maurice Tucker  
Spacecraft and Missiles Res.

Lockheed Aircraft Corporation  
Missiles and Space Division  
7701 Woodley Avenue  
Van Nuys, California  
Attention: Library

Lockheed Aircraft Corporation  
Marietta, Georgia  
Attention: Dr. W. F. Jacobs  
Aerodynamics Dept. -72-07

Marquardt Aircraft Company  
P. O. Box 2013 - South Annex  
Van Nuys, California  
Attention: Technical Library

The Martin Company  
Baltimore 3, Maryland  
Attention: Mr. K. Jarmolow  
Mail No. J-3033  
Attention: Dr. Mark V. Morkovin  
Mail No. J-3033

McDonnell Aircraft Corporation  
Lambert-Saint Louis Municipal Airport  
P. O. Box 516  
St. Louis 66, Missouri  
Attention: Mr. Kendall Perkins

The RAND Corporation  
1700 Main Street  
Santa Monica, California  
Attention: Librarian  
Attention: Dr. Carl Gazley, Jr.  
Attention: Mr. E. P. Williams  
Aero-Astronautics Dept.

Republic Aviation Corporation  
Farmingdale, Long Island, New York  
Attention: Engineering Library  
Attention: Mr. R. W. Perry  
Chief, Re-Entry Simulation  
Lab., Applied Research and  
Dev.

Space Technology Laboratories, Inc.  
P. O. Box 95001  
Los Angeles 45, California  
Attention: Technical Information Center  
Document Procurement  
Bldg. C, Room 2412  
Attention: Dr. James E. Broadwell  
Aerodynamics Research Section  
Attention: Dr. C. B. Cohen  
Attention: Dr. Louis G. Dunn, President  
Attention: Dr. Andrew G. Hammitt, Head  
Aerodynamics Research Section  
Attention: Mr. Ernest I. Pritchard  
Attention: Dr. George E. Solomon

Sperry Utah Engineering Laboratory  
Division of Sperry Rand Corporation  
322 North 21st Street West  
Salt Lake City 16, Utah  
Attention: Mr. Malcolm L. Matthews

Systems Corporation of America  
1007 Broxton Avenue  
Los Angeles 24, California  
Attention: Dr. Paul D. Arthur

United Aircraft Corporation  
Research Laboratories  
East Hartford 8, Connecticut  
Attention: Mr. John G. Lee

#### Internal

Mr. Paul E. Baloga  
Dr. George Bienkowski  
Dr. Gordon L. Cann  
Dr. Julian D. Cole  
Dr. Donald E. Coles  
Dr. Anthony Demetriades  
Dr. Toshi Kubota  
Professor Lester Lees  
Dr. H. W. Liepmann  
Dr. Clark B. Millikan  
Dr. Barry L. Reeves  
Dr. Anatol Roshko

Dr. Frank E. Marble  
Dr. S. S. Penner  
Dr. W. D. Rannie  
Dr. Edward Zukoski

Dr. Harry Ashkenas  
Mr. George Goranson  
Dr. James M. Kendall  
Dr. John Laufer  
Dr. Thomas Vrebalovich  
Mr. Richard Wood

Aeronautics Library (2)  
Hypersonic Files (3)  
Hypersonic Staff and Research Workers (20)



